FLAME CHARACTERIZATION IN DOMESTIC GAS BOILERS

A Thesis Submitted to
the Graduate School of Engineering and Sciences of
İzmir Institute of Technology
in Partial Fulfillment of the Requirements for the Degree of

MASTER OF SCIENCE

in Mechanical Engineering

by
Mustafa Can YENİGÜN

June 2018
İZMİR

We approve the thesis of **Mustafa Can YENİGÜN**

Examining Committee Members:

Asst.Prof.Dr. Alvaro DIEZ
Department of Mechanical Engineering, İzmir Institute of Technology

Assoc.Prof.Dr. Ünver ÖZKOL
Department of Mechanical Engineering, İzmir Institute of Technology

Assoc.Prof.Dr. M. Turhan ÇOBAN
Department of Mechanical Engineering, Ege University

28 June 2018

Asst.Prof.Dr. Alvaro DIEZ
Supervisor, Department of Mechanical Engineering
İzmir Institute of Technology

Prof.Dr. Metin TANOĞLU
Head of the Department of
Mechanical Engineering

Prof.Dr. Aysun SOFUOĞLU
Dean of the Graduate School of
Engineering and Sciences

ACKNOWLEDGMENTS

I would like to express my gratitude to my advisor, Dr. Alvaro Diez, for his guidance, support and patience. The door to his office was always open whenever I had a question about my research.

I would like to thank Dr. H. Murat Altay and M. Saim Kırgız for supporting my experimental work in Bosch. I would also like to thank my colleagues in Bosch TT-RHW/EAP1.2-Man Condensing Appliance Development Team for their help in the lab and the good memories.

I am very grateful to my family, Cemal, Nurten and Onur Yenigün, for the unconditional love and support they have given me throughout my whole life.

Finally, I would like to offer my special thanks to Cüneyt Çankaya, for his endless support in the realization of this study, for his engineering approach which has significant influence on me; but most importantly for his invaluable friendship. Without him, this study would not have been possible.

ABSTRACT

FLAME CHARACTERIZATION IN DOMESTIC GAS BOILERS

In the last decades, pollutant emissions from burning fossil fuels have become of great public concern due to their impact on health and the environment. For this reason, strict legislations have come into force worldwide, which obligate to reduce these emissions. For heating devices such as boilers, it has been realized that these emissions' reduction could be effectively done with the concept of lean premixed combustion. However, lean premixed combustion technology is more vulnerable to the interactions with system acoustics, which brings a negative side effect: Thermoacoustic instabilities.

Thermoacoustic instabilities occur from the feedback loop between the heat release and the acoustic waves in the complete system. They can lead to unwanted noise, flame extinction and, in extreme cases, structural damages. In domestic boilers, these instabilities show themselves as loud noise and flame extinction. In order to eliminate thermoacoustic instabilities in domestic boilers, the trial and error method is used commonly, which requires significant amount of effort and time. Therefore, the researches are focussing on predicting these instabilities at the early stages, where the flame characterization is an important part of the prediction of the thermoacoustic instabilities.

In this study, the flame characterization of the burners used in domestic gas boilers is done experimentally. The Flame Transfer Function method is employed, which is a popular approach for the characterization of the flame response to acoustic perturbations. First, an experimental setup is built, where the velocity fluctuations of the fuel/air mixture and the heat release fluctuations from the flame could be measured. Then, the effects of different parameters, i.e. equivalence ratio, gas quality, perturbation amplitude and burner type on the flame response are investigated.

ÖZET

EV TİPİ GAZLI ISITICILARDA ALEV KARAKTERİZASYONU

Son yıllarda, fosil yakıt yakma sonucunda ortaya çıkan kirletici emisyonlar, insan sağlığına ve çevreye olan etkileri nedeniyle endişe uyandırmaya başlamıştır. Bu nedenle, bu emisyonların azaltılması için dünya çapında katı yasalar çıkarılmaktadır. Kombi gibi ısıtma cihazlarında, emisyonların etkin bir şekilde azaltılmasının ancak fakir önkarışımlı yanma ile mümkün olduğu anlaşılmıştır. Fakat; fakir önkarışımlı yanma teknolojisi, sistem akustiği ile etkileşime eğilimli olduğundan dolayı olumsuz bir yan etkiyi de beraberinde getirmektedir: Termoakustik düzensizlikler.

Termoakustik düzensizlikler, ısı salınımı ve sistemdeki akustik dalgalar arasındaki geri besleme döngüsünden meydana gelmektedir. İstenmeyen gürültülere, alev sönmesine ve ileri durumlarda yapısal hasarlara neden olabilirler. Bu düzensizlikler, ev tipi gazlı ısıtıcılarda (kombilerde) yüksek gürültü ve alev sönmesi olarak görülebilir. Ev tipi gazlı ısıtıcılardaki termoakustik düzensizlikleri önlemek için, yüksek efor ve zaman gerektiren deneme yanılma yöntemi kullanılmaktadır. Bu nedenle, araştırmalar bu düzensizlikleri daha erken safhalarda tahmin etme üzerine yoğunlaşmıştır. Burada, alev karakterizasyonu termoakustik düzensizlikleri tahmin etmede önemli bir rol oynamaktadır.

Bu çalışmada, ev tipi gazlı ısıtıcılarda kullanılan brülörlerin alev karakterizasyonu deneysel olarak yapılmıştır. Alevin akustik düzensizliklere karşı gösterdiği davranışı karakterize etmek için popüler bir yaklaşım olan Alev Transfer Fonksiyonu yöntemi kullanılmıştır. Öncelikle, yakıt/hava karışımındaki hız dalgalanmalarını ve alevdeki ısı salınımı dalgalanmalarını ölçebilmek için deneysel test düzeneği kurulmuştur. Daha sonra, yakıt/hava karışım oranı, gaz kalitesi, pertürbasyon genliği ve brülör tipi gibi farklı parametrelerin alevin tepkisine olan etkisi araştırılmıştır.

TABLE OF CONTENTS

LIST OF FIGURES

Figure **Page**

LIST OF SYMBOLS

C_p	Specific heat at constant pressure
C_v	Specific heat at constant volume
e	Specific internal energy
e'	Acoustic energy density
f	Forcing frequency
p	Pressure
q	Heat release rate
R	Rayleigh index
S_L	Laminar burning velocity
T	Absolute temperature
u	Velocity
γ	Specific heat ratio
ω_*	Reduced frequency
ϕ	Equivalence ratio
ρ	Density
$\mathbb{R}$	Specific gas constant
$\top$	Period of oscillation
$\mathbb{T}$	Time lag

Superscripts

$'$	Fluctuating component
$\bar{}$	Mean value

CHAPTER 1

INTRODUCTION

1.1. Domestic Gas Boilers and Thermoacoustic Instabilities

The increasing energy demand is one of the major challenges in the modern world. Most of this energy need is provided from applications, which include combustion processes. In the last decades, pollutant emissions from these combustion processes have become of great public concern due to their impact on health and the environment. In order to meet stringent nitrous oxides (NO_x) emission legislations and achieve higher thermal efficiencies, the concept of lean premixed combustion has been widely adopted. However, as a negative result of this approach is the appearance of thermoacoustic instabilities.

Thermoacoustic instabilities occur from self-sustained oscillations, forming as a result of the coupling between unsteady heat release and acoustic mode of the system. Thermoacoustic instabilities are unwanted since they can lead to flame extinction, loud noise and in some cases structural damage. In domestic gas boilers, these instabilities show themselves as loud noise and flame extinction, which must be eliminated during the development phase.

Domestic gas boilers are commonly used for space heating and hot water supply. Therefore, they are designated as combination boilers, as its short form, ”combi”. In a domestic gas boiler, the fuel is combusted and the flue gases resulting from combustion process flow through a heat exchanger where the heat of the flue gas is transferred to the water circulating around the heat exchanger. This heated water is used for either space heating or hot water supply. Domestic gas boilers are categorized as conventional and condensing boilers, according to the concept of the combustion technology. In conventional boilers, a diffusion flame is used, where the combustion chamber is directly open to the flue. Due to the low thermal efficiencies and high emission levels, the usage of the conventional boilers are decreasing rapidly. On the contrary, condensing boilers are replacing the conventional boilers due to their higher thermal efficiencies and lower emissions levels, where the latent heat in the flue gases is used as well by condensing the water

vapour in the flue gas to transfer more heat to the water. In condensing boilers, the lean premixed combustion technology is adopted, in order to meet the NO_x emission requirements. However, due to the concept of lean premixed combustion and closed acoustic system, condensing boilers are more vulnerable to the thermoacoustic instabilities.

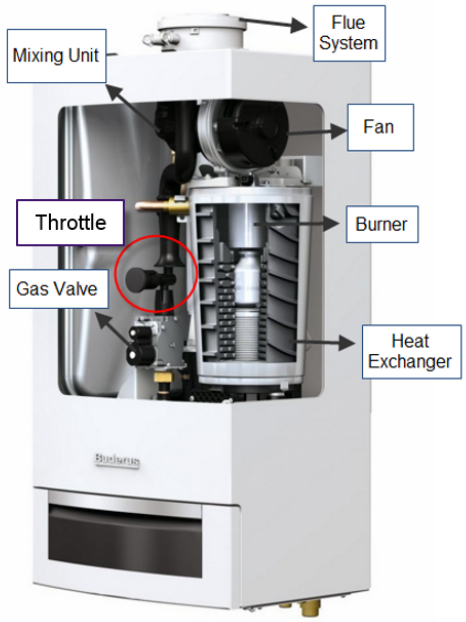

Figure 1.1. Buderus Logamax plus GB172 condensing boiler

Thermoacoustic instabilities are one of the main challenges in the development of the condensing boilers. It causes undesirable noises and flame extinction, therefore they must be eliminated during development phase of the boiler. Since the introduction of ErP (Energy related Products) Directive in Europe and Turkey, the requirements for the emissions and the energy consumption of the products, which use fossil fuels has become more strict. In order to achieve lower emissions and energy consumption, boiler manufacturers started to increase the modulation range of the boiler power. This means, burner load can vary from very low powers to higher powers continuously e.g. between 3 and 30 kW, where they used to operate much lower modulation range in the past. Within this lower range, noise problems caused by combustion instabilities could be solved by trial and error methodology. However, with increased modulation range, additional thermoacoustic instabilities are triggered since the burner operates at a wider load range. In this case, the development time and effort of the heat cell increase significantly with trial and error approach. If any thermoacoustic instability is encountered during this development time,

software and hardware changes (e.g. adding Helmholtz resonators) might be required for suppressing the noise and as a result of these changes, the verification process has to start from the beginning.

Considering these reasons, prediction of the thermoacoustic instabilities at the early stages of the development will save significant amount of time and effort. In that point, the flame characterization is an important part of predicting the possible thermoacoustic instabilities. In this study, the flame transfer function approach is used in order to characterize the flame. This approach has been widely used by many researchers, which is reviewed in the literature survey of the thesis.

1.2. Aim of the Thesis

The aim of this study is, firstly to build an experimental setup where the velocity fluctuations of the fuel/air mixture and the heat release fluctuations from the flame can be measured, and then to show the flame response to the acoustic perturbations within the system, under different conditions affecting the flame response, i.e. different equivalence ratios, burner types, perturbation amplitudes and limit gases. The flame response shows the susceptibility of the flame to resonances, described by the gain and phase of the flame transfer function. The outline of the thesis is as follows:

In Chapter 2, the literature review done for this study is presented. Firstly, the history of the thermoacoustic instability research is introduced and the Rayleigh criterion is derived analytically. Then, thermoacoustic instabilities are explained in thermodynamic cycles to get a better understanding. The concept of the Rijke tube is explained as a convenient example to study thermoacoustics. A detailed review is given for the flame characterization and the Flame Transfer Function method is described, which is used to show the response of the flame to acoustic oscillations. Finally, the chemiluminescence method for heat release measurements are explained and a literature review is presented.

In Chapter 3, the methodology of the study is given. The development of the experimental methods and the details of the experimental setup for the determination of the flame transfer function are explained. The schematic of the experimental setup is given and as well as the explanation of its components. Then, the operation mode of the test rig setup is described step by step. Finally, the post-processing method of the data

collected from the experiments is given and calculation of the flame transfer function from processed data is presented.

In Chapter 4, the results of the parametric study of the flame transfer function are presented. The influence of the flame and burner parameters such as equivalence ratio, limit gases, perturbation amplitude, burner types and burner parts on the flame response is studied. The findings from the experiments are presented in flame transfer function graphs and the results are discussed.

In Chapter 5, the results are summarized and the future studies are explained. The highlights of the results are presented. For the future studies, it is explained that how this study will help for the prediction of the thermoacoustic instabilities.

CHAPTER 2

LITERATURE REVIEW

Combustion driven oscillations have been studied in the literature for the last two centuries. With the introduction of the lean premixed combustion technology, they became one of the major problems in condensing boiler development as well. In this chapter, the history of the thermoacoustic instability research is introduced and the literature review is given for the flame characterization study.

2.1. Thermoacoustic Instabilities

Combustion oscillations were first observed by Higgins in 1777, reported as "singing flames" [1]. He showed that he could produce noise, by placing a hydrogen diffusion flame inside a glass tube. He observed different tones by changing the width, length and thickness of the tube. In 1859, Rijke discovered that sound could be generated when a heated gauze, which was made of iron wire, was placed inside a vertical glass tube at a distance of one-fourth of its entire length from the lower end [2]. He suggested that when warming of gauze was stopped, an ascending current of air was established passing through the meshes of the wire gauze where the air was heated and consequently expanding. After this expansion, a contraction succeeded immediately due to the cooling effect of the sides of the tube. He attributed the sound generation to these successive expansions and contractions.

A scientific explanation of the phenomena was published by Lord Rayleigh in 1878, which describes the mechanism where heat release excites pressure oscillations [3]. According to his statement, which is now known as Rayleigh criterion; if the heat is added during compression and removed during expansion, the instability is encouraged. If the heat is removed during compression and added during expansion, the instability is discouraged.

The first to describe this criterion in a mathematical form was Putnam and Dennis [4]:

$$\int_0^{\top} \int_0^{V} p'(x,t)q'(x,t)dvdt > 0 \tag{2.1}$$

Here p' represents the pressure fluctuations and q' represents the heat release fluctuations, $\top$ is the period of oscillation and V is control volume. Additionally, the left-hand side of the inequality is defined as Rayleigh index, R. If the inequality Eq. (2.1) is satisfied (in other words, if R value is positive), thermoacoustic instability occurs. The left-hand side of the inequality indicates the total mechanical energy added to the pressure oscillations from the heat release (amplification of pressure fluctuations) [5].

2.2. Analytical Derivation of the Rayleigh Criterion

Lord Rayleigh's famous criterion is used by many researchers to characterize the heat driven oscillations. In order to derive the mathematical expression of the Rayleigh Criterion, some basic assumptions are used [6]. For the derivation, a tube hosting a flame is taken into consideration, as seen in Figure 2.1.

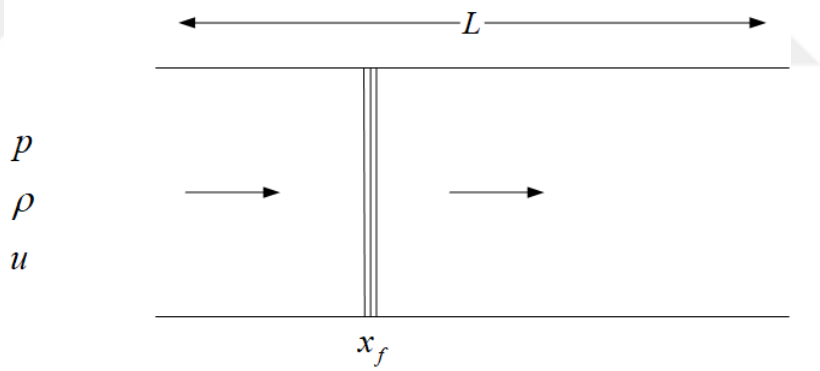

Figure 2.1. One dimensional reacting fluid flow with flame at $x = x_f$

The assumptions for the derivation of conservation equations for the flow in the tube are given as follows:

1. One-dimentional flow, in the longitudinal direction of the tube.
2. Inviscid flow
3. Negligable thermal conductivity to the surroundings

4. Ideal gas

5. Stationary flow

With these assumptions, the acoustic pressure and velocity are obtained with the unsteady heat addition to the acoustic field. In order to get the forced acoustic wave equation, equations are reduced to the case where mean heat release is negligible, i.e. approximately homogeneous field, and when the mean flow is also negligible. The conservation equations for reactive gas dynamics can be expressed as:

$$\text{Mass continuity:} \quad \frac{\partial \rho}{\partial t} + \frac{\partial (\rho u)}{\partial x} = 0 \tag{2.2}$$

$$\text{Momentum:} \quad \rho \frac{\partial u}{\partial t} + \rho u \frac{\partial u}{\partial x} + \frac{\partial p}{\partial x} = 0 \tag{2.3}$$

$$\text{Energy:} \quad \rho \frac{\partial e}{\partial t} + \rho u \frac{\partial e}{\partial x} = -p \frac{\partial u}{\partial x} + q \tag{2.4}$$

where ρ, u, p, e and q are the density, velocity, pressure, specific internal energy and heat release rate per unit volume, respectively.

Taken into consideration the fourth assumption, the gases at the both sides of combustion zone behave as ideal gases, the ideal gas state equation:

$$p = \rho \mathbb{R} T \tag{2.5}$$

where $\mathbb{R}$ is the specific gas constant and T is the absolute temperature.

Combining Eq.(2.2), Eq.(2.4) and Eq.(2.5) (note $e = C_v T,\ \mathbb{R} = C_p - C_v,\ \rho e = \rho C_v T = C_v \frac{p}{\mathbb{R}} = \frac{p}{\gamma - 1}$, where γ is the specific heat ratio), we get:

$$\frac{\partial p}{\partial t} + u \frac{\partial p}{\partial x} + \gamma p \frac{\partial u}{\partial x} = (\gamma - 1) q \tag{2.6}$$

Since only the small perturbations are of interest in the analysis of the thermoacoustic instabilities, the system variables are separated into their mean (function of space only) and small perturbation (function of space and time) components:

$$
\begin{aligned}
p(x,t) &= \overline{p}(x) + p'(x,t) \\
u(x,t) &= \overline{u}(x) + u'(x,t) \\
\rho(x,t) &= \overline{\rho}(x) + \rho'(x,t) \\
q(x,t) &= \overline{q}(x) + q'(x,t)
\end{aligned}
\tag{2.7}
$$

where $\overline{()}$ and $()'$ are the mean and the perturbation of a variable, respectively.

Taken into consideration the stationary flow assumption, the conservation of mean flow can be described as:

$$\text{Mass continuity:} \quad \frac{d}{dx}(\overline{\rho u}) = 0 \tag{2.8}$$

$$\text{Momentum:} \quad \overline{\rho u}\frac{d\overline{u}}{dx} + \frac{d\overline{p}}{dx} = 0 \tag{2.9}$$

$$\text{Energy:} \quad \overline{u}\frac{d\overline{p}}{dx} + \gamma\overline{p}\frac{d\overline{u}}{dx} = (\gamma - 1)\overline{q} \tag{2.10}$$

Substituting the flow variable components in Eq.(2.7) into Eqs.(2.3) and (2.6) and neglecting second order terms of fluctuating components, linear governing equations are obtained for the perturbations:

$$\overline{\rho}\frac{\partial u'}{\partial t} + \overline{\rho u}\frac{\partial u'}{\partial x} + \overline{\rho}u'\frac{\partial \overline{u}}{\partial x} + \rho'\overline{u}\frac{\partial \overline{u}}{\partial x} + \frac{\partial p'}{\partial x} = 0 \tag{2.11}$$

$$\frac{\partial p'}{\partial t} + \overline{u}\frac{\partial p'}{\partial x} + u'\frac{\partial \overline{p}}{\partial x} + \gamma\overline{p}\frac{\partial u'}{\partial x} + \gamma p'\frac{\partial \overline{u}}{\partial x} = (\gamma - 1)q' \tag{2.12}$$

Introducing the acoustic energy density, e', which is derived from the unforced conservation equations for a one-dimensional acoustic field [7]:

$$e' = \frac{\overline{\rho}u'^2}{2} + \frac{p'^2}{2\overline{\rho c}^2} \tag{2.13}$$

where the first term in the right-hand side is the kinetic acoustic energy and the second term is the potential acoustic energy.

Linear governing equations Eq.(2.11) and Eq.(2.12), for a zero mean velocity and for no spatial change in the mean variables, can be written as:

$$\overline{\rho}\frac{\partial u'}{\partial t} + \frac{\partial p'}{\partial x} = 0 \tag{2.14}$$

$$\frac{\partial p'}{\partial t} + \gamma\overline{p}\frac{\partial u'}{\partial x} = (\gamma - 1)q' \tag{2.15}$$

Multiplying Eq.(2.14) by u' and Eq.(2.15) by $\frac{p'}{\gamma\overline{p}}$, and summing these two terms and using Eq.(2.13), we obtain:

$$\frac{\partial e'}{\partial t} + u'\frac{\partial p'}{\partial x} + p'\frac{\partial u'}{\partial x} = \frac{\gamma - 1}{\overline{\rho c}^2}p'q' \tag{2.16}$$

Integrating Eq. (2.16) temporally, over the period of oscillation, $\top$, and spatially, over the length of the combustor, L, we get:

$$\Delta_\top \int_0^L e'dx = \frac{\gamma - 1}{\overline{\rho c}^2}\int_0^\top \int_0^L p'(x,t)q'(x,t)dxdt - \Delta_L \int_0^\top E'dt - \int_0^\top \int_0^L \Phi(x,t)dxdt \tag{2.17}$$

where $\Delta_\top$ and Δ_L are the changes over time and length, respectively. The left-hand side of Eq. (2.17) represents the change in the acoustic energy per cross-sectional area of the combustor. The first term in the right-hand side is the Rayleigh index (which is given in Eq. (2.1)), the second term is the acoustic energy flux through the control surface of the field which is defined $E' = p'u'$, the third term expresses the dissipation in the acoustic field. In Eq. (2.17), it is seen that when Rayleigh index is positive, i.e. p' and q' are in-phase, and it is large enough to overcome both dissipation and the energy flux terms (second and third term in the right-hand side), there will be an increase in the acoustic energy in the combustor and thermoacoustic instability will occur.

2.3. Thermodynamic Interpretation of Thermoacoustics

Thermoacoustic instabilities can be explained better in terms of a thermodynamic cycle [8]. Consider a gas, compressed and expanded by a standing acoustic wave. Since sound waves are isentropic, volume moves back and forth on an isentrope in a p-v diagram shown in Figure 2.2, where dashed grey lines represent constant entropy. Pressure (—) and velocity fluctuations (- - -) can also be seen on the right top side. If heat is added and extracted periodically to the gas, there is an increase in specific volume v of the gas

and if the heat addition is in-phase with pressure fluctuations (as seen in Figure 2.2 right-middle), the state of gas volume moves clockwise on a thermodynamic cycle, following the curve 1-2′-3′-4′. This can be called as "thermoacoustic heat engine" where mechanical energy is transferred into sound wave and a self-excited instability may occur. If heat addition and pressure fluctuations are not perfectly in-phase, the area of cycle 1-2′-3′-4′ will be smaller, therefore the efficiency of the engine will decrease. In the case where heat release fluctuations are out-of-phase with pressure fluctuations (as seen in Figure 2.2 right-bottom), system follows the cycle 1-2″-3″-4″ and mechanical energy is extracted from the acoustic wave.

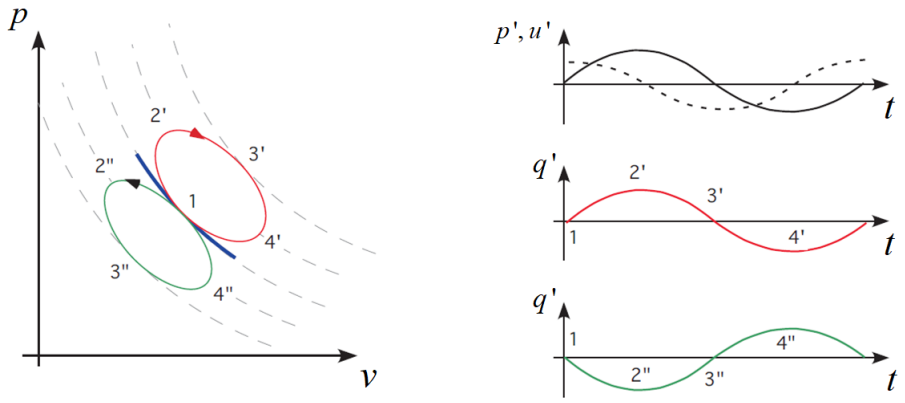

Figure 2.2. Thermodynamic interpretation of Rayleigh's stability criterion [8].

The mechanical work performed by the acoustic perturbations with heat release can be formulated as follows:

$$\oint pdv = \oint (\bar{p} + p')d(\bar{v} + v') = \oint \bar{p}dv' + \oint p'dv' = 0 + \oint p'dv' = \oint p'dv' \quad (2.18)$$

If the change in specific volume v' is split into an isentropic part, where $v' = -vdp'/\gamma p'$ (γ is specific heat ratio) and a part $v'^{(q)}$ from heat addition or removal:

$$\oint p'dv' = -\frac{v}{\gamma p}\oint p'dp' + \oint p'dv'^{(q)} = 0 + \oint p'\frac{dv'^{(q)}}{dt}dt \sim \oint p'q'dt \quad (2.19)$$

The rate of change of $v'^{(q)}$ term with respect to time is proportional to fluctuations in heat release. It can be concluded that energy is added to acoustic field by the work performed by "thermoacoustic engine", if the Rayleigh index is positive. However, if the

acoustic losses in the system exceed the rate of energy input caused by fluctuating flame, a self-excited instability cannot develop, even the Rayleigh index is positive.

2.4. Rijke Tube

Thermoacoustic instability is a complex phenomenon and some simplified models are needed to understand its nature. The Rijke tube is a convenient example to study thermoacoustic instabilities. The Rijke tube is simply a cylindrical duct with both ends open and a heat source placed inside it, typically a heated gauze. The tube is positioned vertically and both ends of the tube are open. When the heated gauze is placed at the lower part of the tube (specifically a quarter of the tube length from the bottom), air flows through the tube upwards due to natural convection and it causes self-excited acoustic oscillations. When the heated gauze is placed at the upper half of the tube, acoustic oscillations are damped. This can be explained by evaluating the acoustic pressure and velocity modes in the tube. In the first mode, the pressure nodes are located at the ends of the tube. At the same locations, the velocity antinodes are located, where the velocity node is located at the middle of the tube.

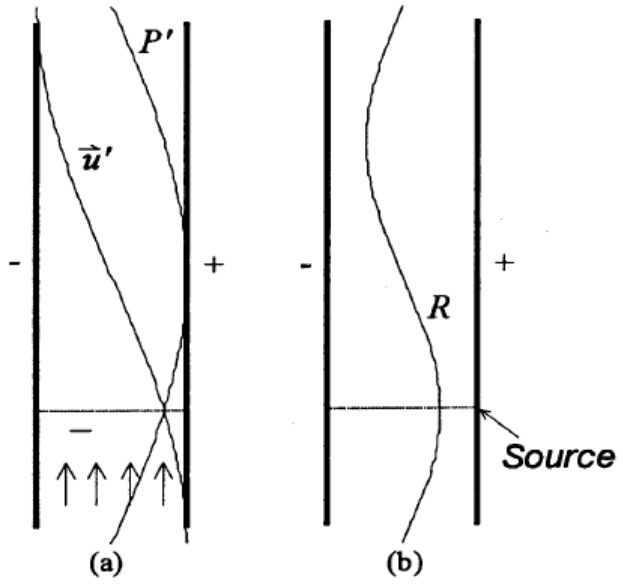

Figure 2.3. Schematic of a Rijke tube depicting the first mode instability (a) Pressure and velocity mode shape (b) Rayleigh index [9]

When the lower part of the tube is heated, the phase of velocity is 90° ahead of the phase of the pressure and there is a few degrees of phase delay of heat release with respect to the phase of velocity. In this way, the Rayleigh index is positive and oscillations are self-excited. If the upper part of the tube is heated, the phase of the velocity is 90° behind of the phase of the pressure oscillations, heat release oscillations are even more delayed. This leads to a negative Rayleigh index, where the system is damped by the heat source [5].

Bosscha and Riess inverted the effect of the Rijke tube [10], [11]. They produced oscillation by placing refrigerated gauze in the upper part of the tube and forcing upward convection of hot air. In this case, the Rayleigh index was positive and oscillations were self-excited.

The Rijke tube has been studied by many researchers. A detailed review of thermoacoustic devices related to the Rijke tube are given by Raun et. al. [12]. In their paper, they explained the mechanisms of heat-driven acoustic oscillations, discussed experimental works with Rijke tubes and burners and the validity of the Rayleigh criterion with these experiments. It was shown that the Rayleigh criterion is a valid explanation for the thermoacoustic instabilities, where the heat-driven oscillations have been predicted successfully. It was confirmed from various studies in the review that the first mode of a Rijke tube can be achieved by placing the heated gauze at one-quarter of the tube length from the bottom. It was also shown that in order to drive other harmonics, the heater must be placed at other positions in the tube. In addition, they also review the mathematical analyses of acoustic oscillations in Rijke-type devices, beginning with the equations for mass, momentum and energy conservation. The response of the heat source to the acoustic oscillations were modeled showing that the response model has a significant effect on the predicted growth rate, where they do have less effect on predicting the resonant frequencies.

Carvalho et al. presented an analysis that defined the location of the heater to drive maximum amplitude acoustic oscillations in a Rijke tube [13]. They developed a mathematical model based on the Rayleigh criterion and validated their model experimentally. For a Rijke tube of length L, they calculated theoretically that the maximum amplitude oscillations occurred when the heater was placed to $L/4$ for the fundamental mode, where it was experimentally verified. They validated their mathematical model also for second and third harmonics.

2.5. Flame Characterization in Thermoacoustic Instabilities

The response of the flame to acoustic perturbations has an important role in combustion driven oscillations. In a combustion system, such as a domestic gas boiler, in addition to the total acoustic system of the heat cell, burner and flame characteristics are the main contributors to thermoacoustic stability of the system. In order to better understand the phenomena leading the instability and propose solutions to predict them, it is important to determine the flame response to acoustic perturbations. One of the common methods to characterize the flame response to acoustics is the Flame Transfer Function (FTF).

The idea to use the transfer function to characterize the flame response to acoustic perturbations originates from the approach in the system control theory. In a system control problem, the system is considered as a black box. In this case, the flame or the burner is considered as a black box which transforms the input signal – oscillations of flow velocity to output signal – oscillations of heat release rate. In the simplest case, when u' and q' are an harmonic function of single frequency f, the transfer function can be expressed as [14]:

$$G(f) = \frac{q'(f)/\overline{q}}{u'(f)/\overline{u}} \tag{2.20}$$

where the ratio $\overline{q}/\overline{u}$ of the mean heat release rate to the mean velocity is introduced to normalize the transfer function and to make it dimensionless. That means, the transfer function is the ratio of relative flame response to the relative acoustic perturbation and it characterizes the flame heat release rate susceptibility to the acoustic velocity oscillations.

A popular approach to represent the Flame Transfer Function is the so-called $(n-\tau)$ representation. In this approach, n represents the sensitivity of the heat release rate to the pressure oscillations and τ is the phase lag between pressure oscillation and the corresponding heat release oscillation. Since the acoustic pressure and velocity oscillations are coupled, n is related to the gain of the transfer function, where the phase lag τ related to the phase delay between the excitation and response oscillation. The transfer function is a complex number and can be characterized with its magnitude (gain) and phase. The flame response is the indicator of the susceptibility of the flame to flow perturbations, therefore it could give the idea that where resonance might occur. In other words, the gain

indicates the growth rate of the thermoacoustic instability, where the phase shows the sign of the growth rate.

Fleifil et al. developed an analytical model to describe the response of a laminar premixed flame to velocity oscillation [15]. In their model, they showed that the magnitude of the heat release fluctuation and its phase with respect to the pressure oscillation depend primarily on the flame Strouhal number, which is the ratio of the dominant frequency times the tube radius to the laminar burning velocity (S_L). It was found that the high frequency oscillations did not have any significant effect on the heat release rate, whereas low frequency oscillations did have a strong effect. In the opposite way, the time delay was maximum at high frequencies and minimum at low frequencies. Their model was also supported with the experimental results of Blackshear [16], where the flame area perturbation is directly proportional to the normalized velocity perturbation and the time delay is dependent on the flame Strouhal number. Ducruix et al. extended the model proposed by Fleifil et al. to a more general situation in their study, by taking the flame angle into account [17]. It was shown that the amplitude and phase of the flame transfer function could be described in terms of the reduced frequency ω_*, where it was derived as:

$$\omega_* = Rf/S_L cos\alpha_0 \tag{2.21}$$

where f is the driving frequency,
R is the burner radius,
S_L is the laminar burning velocity,
α_0 is the half-cone angle of the steady flame (Figure 2.4).

The transfer function was compared with experimental data consisting of different equivalence ratios and two different burner diameters, and good agreement was obtained for low values of the reduced frequency. However, for intermediate and large frequencies, there were large differences in phase, compared to the analytical model due to the assumptions done for the velocity field in the fresh gases side. In order to determine the flame transfer function experimentally, the flame heat release and the velocity at the burner exit were measured. CH* radicals were measured by using a photomultiplier tube (PMT) to account for heat release rate. For the velocity measurement at the burner outlet, Laser Doppler Velocimetry (LDV) was used.

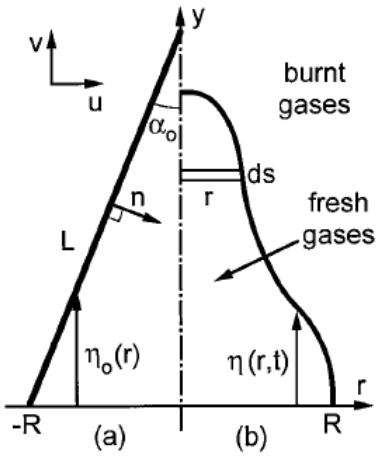

Figure 2.4. Sketch of the flame and flow parameters (a) in the steady situation and (b) in the perturbed situation. [17]

Schuller et al. showed the importance of the description of the perturbed velocity field on the flame front when dealing with the flame transfer function [18]. In this study, the phase shift was taken into account, which was caused from the convection of the harmonic velocity perturbation produced at the burner outlet to the flame front by the mean flow. With their new velocity model, the flame response could be represented at wider range of frequencies. In their experimental studies, the velocity field of the fresh reactants was measured by particle image velocimetry (PIV). Cuquel et al. studied the response of the conical premixed flames to velocity perturbations for different flow operating conditions, with and without the presence of a flame tube to confine the reaction zone [19]. They introduced a new convective model to determine the flame transfer function and obtained an analytical expression, which matched previous models at low and high frequencies. The results were compared with experimental data, which showed good agreement for the phase. In the experiments, the flame height was modified, either through a change in the flow velocity or burning velocity. Results showed that the laminar burning velocity has greater influence on the flame response than the flow velocity in the cases considered in this study, which was the result of the dependence of ω_* on flow velocity for elongated flames, for which $cos\alpha \simeq 1$. It was also shown that the analytical model overpredicted the gain in the absence of the flame tube where the difference is reduced in the presence of the flame tube. Schreel et al. analysed the flame response of two different types of flame holders against acoustic perturbations and showed the frequency

dependence of the transfer function [20]. It was found that there was resonance at about 150 Hz with a perforated brass burner, where it was observed from the gain of the transfer function. The significant effect of the standoff distance of the flame was also shown, which was directly affected by the temperature of the flame holder. It was observed that the resonance frequency was shifted even with a small temperature change of 40 K in flame holder temperature. As a more complex way, it was also shown that the acoustical behaviour could be changed by changing the flow velocity.

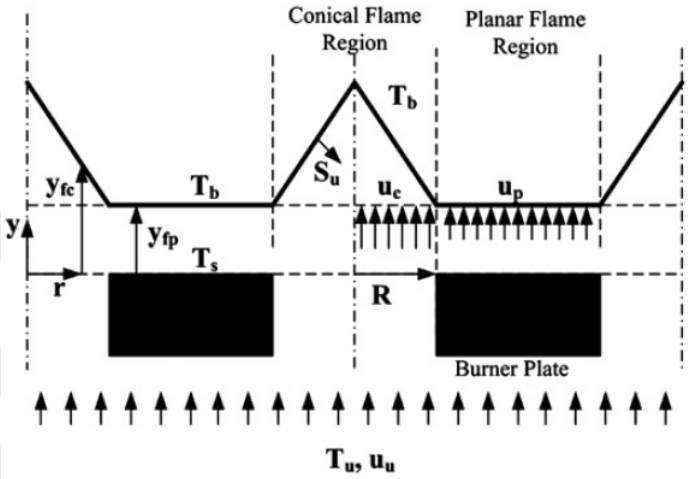

Figure 2.5. Flame surface in perforated-plate stabilized burner [21]

Altay et al. studied the dynamic response of a laminar perforated-plate stabilized flame under different power and equivalence ratios by extending previous planar flame models to include the conical flame surfaces [21]. It was found that when the equivalence ratio was increased, the flame got closer to the burner surface, increasing burner plate surface temperature and the resonant frequency. By increasing the inlet velocity, it was found that the flame area increased causing heat release oscillations at higher frequencies than resonant frequency. At low frequencies, no effect of increasing the inlet velocity on the resonant frequency and the heat release rate response was observed, since they were controlled mainly by the burning velocity oscillations associated with the heat loss from the flame to the burner plate surface. The model was compared with the experimental measurements, where good agreement was obtained. Kornilov et al. analysed the thermoacoustic behaviour of multiple flame burner decks [22]. Their approach was to decompose the flame transfer function into individual flames or subsystems of the burner and represent the total flame transfer function as their weighted sum. It was found that the

perforation pattern and perforation hole diameter were the governing parameters of the transfer function and concluded that the superposition of the transfer functions of unisize perforations have a good agreement with the transfer function of the multi-size perforations, if both were measured with the burner deck which has the same porosity. It was observed that the gain and phase of the transfer function were strongly affected from the hole diameter, where the distance between holes have a great impact on the phase of the transfer function as well.

Kornilov et al. measured the flame response of a multi-slit Bunsen burner experimentally and investigated the effects of the mean flow velocity, the equivalence ratio and the slit configuration on the flame transfer function [23]. Their experimental setup consisted an enclosed vessel with a flat perforated disk where methane and air mixture was given from a mass flow controller. It was found that the frequency range where the gain exceeds 1, increased by increasing the velocity. Changing the velocity had no effect on the slope of the phase, since the phase was proportional to the convective time H/u and the laminar flame height H also increased when the flow velocity u increased. Only the saturation level of the phase increased with velocity, since the cutoff frequency shifted to higher frequencies. On the other side, the slope of the phase decreased for increasing equivalence ratio ϕ, since the flame height H was smaller, which was a result of higher burning velocity of a richer mixture. An increase in slit width of the burner plate corresponded to an increase in flame height whilst the flow velocity remained constant, which caused steeper slope of the phase. Increasing the distance between the slits of the burner plate caused a separation of the flame anchoring points and a larger flame height. In this case, the slope of the phase increased, where the gain was scarcely influenced. See their article for detailed review of the experimental studies of thermoacoustic models of premixed Bunsen burners.

Durox et al. analysed non-linear flame transfer functions for different flame geometries [24]. The Flame Describing Function (FDF) was used to account for the flame non-linearity, an extended version of the transfer function, which depends on the amplitude of the input perturbations. The effects of the disturbance amplitude on the gain and phase were investigated for different flame geometries including a conical flame, "V" flame, "M" flame and perforated-plate stabilized small conical flames, shown in Figure (2.6). For perforated-plate stabilized flames, very high levels of perturbation were reached without any flame blow-off comparing with the other flames, since the flames were very

well anchored on the burner. The gain was higher than 1 at low frequencies. These phenomena indicate that for the strong perturbations, the changes in the heat release rate are less important for high frequencies, where the strong perturbations have significant effect for low frequencies. It was also shown that the slope of the phase increased at high disturbance levels.

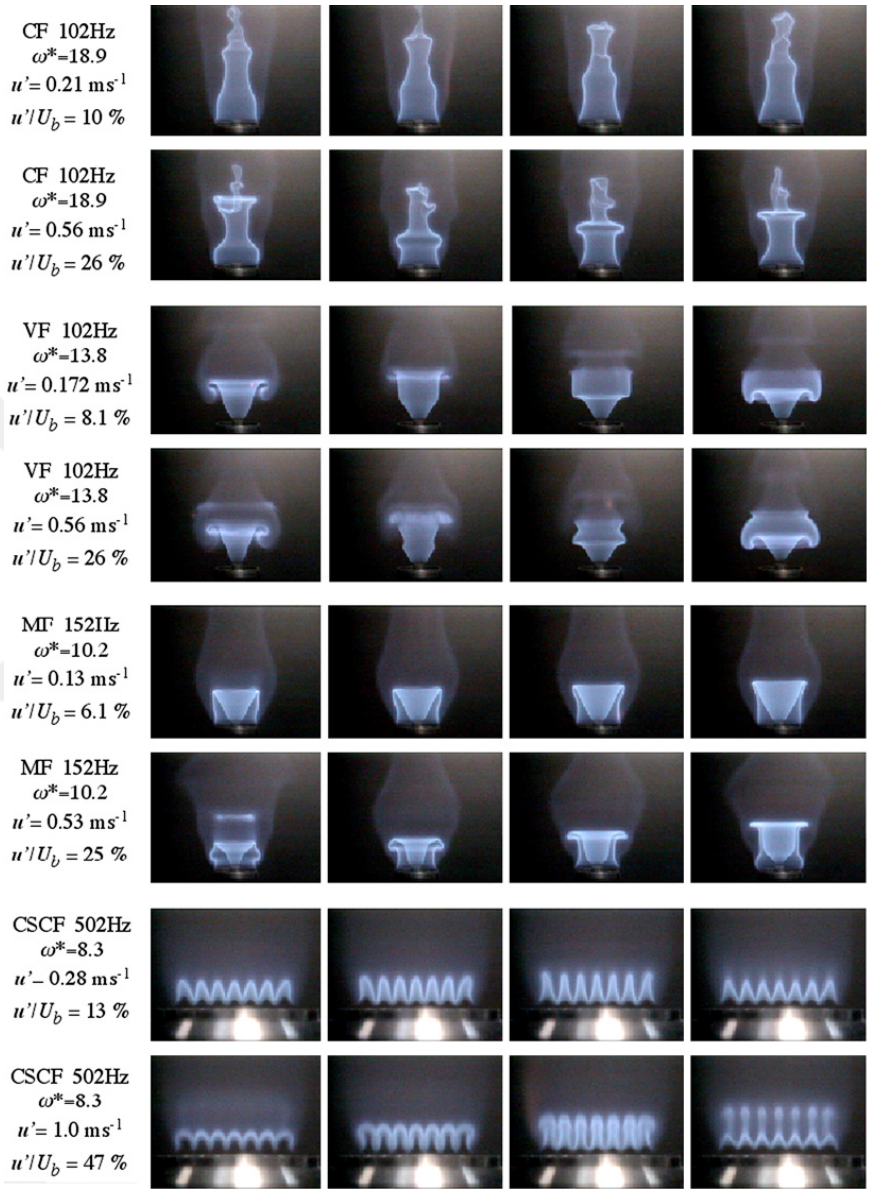

Figure 2.6. Images taken during oscillation for conical flame (CF), ”V” flame (VF), ”M” flame (MF) and collection of small conical flames (CSCF) in different perturbations levels u'/U_b [24]

2.6. Chemiluminescence

Chemiluminescence is the light emitted by molecules created after a chemical reaction, while the molecules are passing from an excited energy state to a lower energy state. In combustion diagnostics, chemiluminescence is widely used as an optical measurement technique and provides information about reaction zone conditions. Particularly, the intensity of OH* and CH* radicals has often been used as a measure of the heat release rate in flame characterization.

In early studies, Clark studied OH*, CO*, CH* and C_2* radiations from propane-air and ethylene-air flames at different equivalence ratios [25]. It was shown that the intensity of CH* emissions measured with photomultiplier tube were very sensitive to the changes in equivalence ratio and initial metered equivalence ratios had a direct relation with measured C_2*-CH* ratios. Price et al. investigated the mechanism of noise generation in the premixed flames by monitoring the intensity of C_2* and CH* emissions with a photomultiplier tube [26]. In their study, it was found that the chemiluminescence intensities measured from premixed flames changed linearly with the total fuel/air mixture rate. The radiated sound pressure level measured with a microphone was compared with calculated values from the chemiluminescence intensity measurements of C_2* radicals, where good agreement was found in between. Higgins et al. took measurements of CH* chemiluminescence from premixed methane/air flame at different equivalence ratios [27]. As in previous studies, it was found that CH* chemiluminescence was linearly proportional to total gas/air mixture rate. In addition, it was suggested that NO_x emissions and thermoacoustic instabilities could be mitigated with an active control algorithm based on CH* chemiluminescence. Hardalupas and Orain conducted detailed measurements of heat release rates and equivalence ratio by using chemiluminescence intensities [28]. In their study, the influence of equivalence ratio on chemiluminescence intensity was shown independent from the fuel flow rate by normalizing the intensity results by the fuel flow rate. The mean intensity of CH* increased as the equivalence ratio increased towards stoichiometry, where the heat release rate was also increased. When the equivalence ratio exceeded 1.1, the mean intensity of CH* started to decrease, since flame extinction limits were approached. Balachandran et al. measured the flame response of a premixed flame with three different approaches: OH* and CH* chemiluminescence measurements, flame surface density (FSD) computation based on OH planar laser-induced fluorescence

(PLIF) imaging, simultaneous OH and CH_2O PLIF imaging [29]. Good agreement was found for the global heat release rate between OH* and CH* chemiluminescence both in gain and in phase, where the FSD based on OH PLIF was found to agree well with chemiluminescence measurements. It was concluded that for the transfer function measurement, the chemiluminescence technique was a good choice, since no additional skills were required for computation and measurements and they were reasonably cheaper.

This method, chemiluminescence intensity of CH* as an indicator of the heat release rate, is widely accepted for the flame transfer function measurements ([14], [17], [19], [21], [23]).

2.7. Summary

In the flame characterization study, the flame transfer function approach is the most common method to show the response of the flame to the acoustic perturbations. Studies show that some flame and burner parameters have greater effect on the flame response, i.e. the flame transfer function. It was shown that the equivalence ratio of the mixture, the burner geometry, the burner perforation pattern and the perturbation amplitude affect the flame response significantly, since they all have effect on the burning velocity and the flame height, which change the response of the flame. Therefore, these parameters are studied in this thesis, in order to show their effects on the flame response.

The common method for the flame characterization in the literature reviewed in this chapter is experimental method. The experimental setup is built accordingly, to mix the fuel and air evenly, to perturb the mixture flow and to visualize the flame where the velocity and heat release fluctuations could be measured.

Thermoacoustic instabilities in boilers have been previously studied within Bosch as well. Parmar made the flame characterization of different burners used in domestic gas boilers experimentally, where he conducted a parametric study by changing the equivalence ratio and the burner load [30]. In addition, the boiler was described as a network of the acoustic elements and the acoustic properties of each element were obtained where the acoustic behaviour of the system was characterized as well. Reijke performed thermoacoustic stability analysis of a condensing boiler, where a stability model is created with the acoustical impedances of the system and flame transfer function [31]. His model predicted

the major unstable frequencies, however it still needs improvement. Manohar focused on the response of different flames to the acoustic perturbations [32]. The flame transfer function was measured by changing various parameters affecting the flame response and correlations between those parameters and the flame transfer function is presented.

In this study, an experimental investigation of the flame characterization in a domestic gas boiler was carried out. This study is part of a scheme for prediction of the thermoacoustic instabilities by means of finding the flame response to the acoustic perturbations. Prediction of the thermoacoustic instabilities play an important role in burner and boiler development, since it saves significant amount of time and effort, unlike the conventional trial and error method. Therefore, burner and boiler manufacturers focus their researches on methods to predict these instabilities, including Bosch. In this investigation, first an experimental setup is built, where the velocity fluctuations in the fuel/air mixture and the heat release fluctuations in the flame could be measured. In order to characterize the flame, the flame transfer function approach is used, which is a common method in the literature. A parametric study is conducted experimentally, to show the effects of flame and burner parameters on the flame response.

CHAPTER 3

METHODOLOGY

In this chapter, the experimental test setup used for the flame transfer function measurements of premixed flame stabilized on perforated burner are explained. The techniques for the heat release rate and velocity measurements are described. Moreover, the post processing methods to obtain the transfer function from the experimental data are explained.

3.1. Experimental Setup

As mentioned in the introduction, the aim of this study is to characterize the flame stabilized on the burner of a domestic condensing boiler by measuring the flame transfer function. The flame transfer function is determined by the response of the flame to the velocity fluctuations, where measurements are needed on the oscillating velocity and heat release. For that purpose, it is necessary to build an experimental test setup where the flame can be stabilized on a perforated plate burner, to adjust the gas/air mixture flow rate and the equivalence ratio, to create velocity perturbations at different frequencies and to process the data with a data acquisition module. While designing this experimental setup, the studies reviewed in the literature survey are benefited.

The schematic of the experimental setup that used in this study is shown in Figure 3.1. The experimental setup consists of a straight tube, a burner used in domestic condensing boilers, a hot-wire anemometer, a photomultiplier tube (PMT), a loudspeaker, an amplifier, a waveform generator, a data acquisition card and mass flow controllers. The test setup is designed to operate with different burners, at different equivalence ratios.

The test setup is built with a tube which is made from aluminium with 90 mm internal diameter, 500 mm height and 5 mm wall thickness. The height was determined so that the tube allows for the mounting of the the loudspeaker and hot-wire anemometer as well as enough length for the proper air and fuel mixing. In order to measure the velocity fluctuations, a hot-wire anemometer is mounted at a distance of 150 mm upstream of

the burner. Mass flow controllers are used to control the fuel and air flow rates, i.e. the equivalence ratio through an in-house built software. The fuel used in the experiments is G20 (naming according to British Standard BS EN 437) unless stated otherwise, which consists of 100% methane.

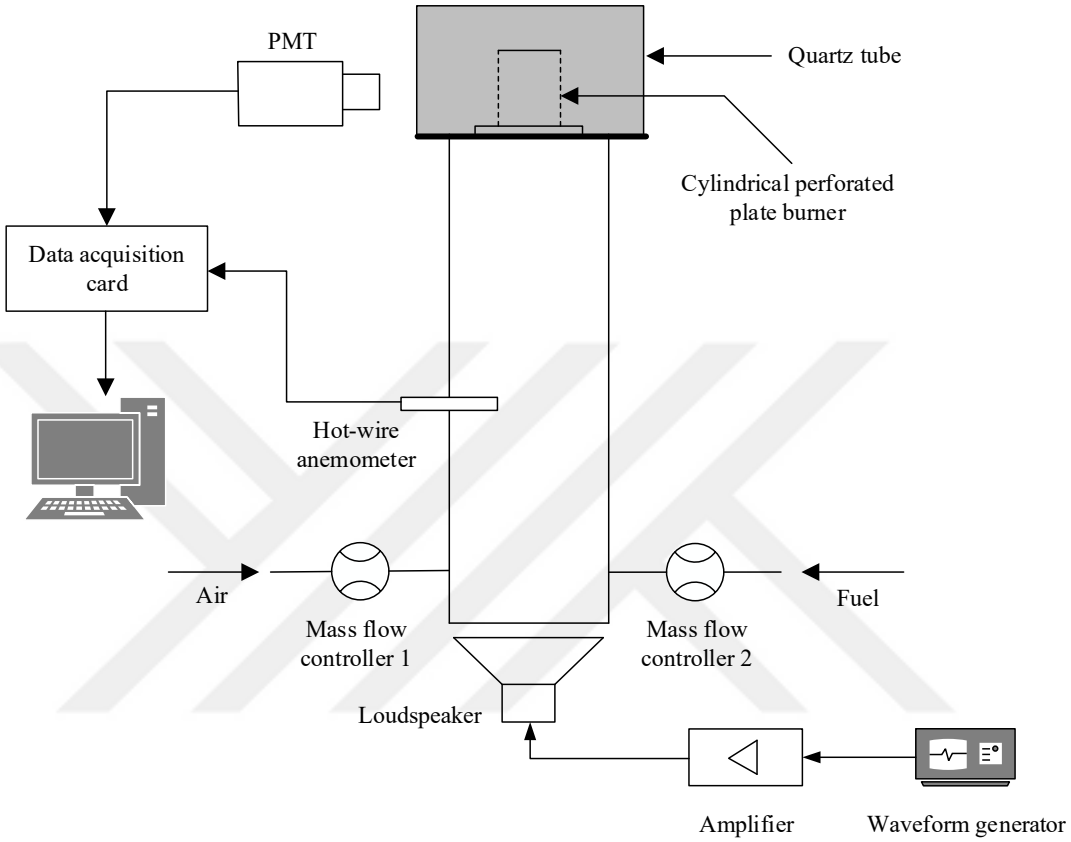

Figure 3.1. Schematic of the experimental setup

The fuel-air mixture is excited with a loudspeaker, which is located at the lower end of the aluminium tube. The loudspeaker is connected to a waveform generator and an amplifier, in order to create perturbation at different frequencies and different amplitudes. At the upper end of the tube, the burner is assembled where the flame is attached. At the surroundings of the burner, a Quartz tube is located, allowing to measure the CH* radicals radiated from the flame which gives the heat release fluctuations. For that purpose, a photomultiplier tube with a CH* filter with the peak wavelength at 420 nm is used for the chemiluminescence measurements of the flame. The measurement data from the hot-wire anemometer and the photomultiplier tube are collected with a data acquisition card, which

is connected to a computer. The software is specially designed for the collection of the measurement data with LabView. The details of the experimental setup and measurement techniques are explained in the following subsections.

3.1.1. Burner

The experiments are conducted with a perforated plate burner (named as sample no.1 in this study), which is used commercially in premixed condensing boilers (Figure 3.2). It consists of regular patterns of holes on the surface, where flame is attached. The combination of the hole patterns of the perforation might change for different types of burners according to the requirements. The material of the burner is stainless steel. Some perforated plate burners might include additional sub-elements, such as a distributor plate for the distribution of the fuel/air mixture.

Figure 3.2. Perforated plate burner

3.1.2. Hot-wire Anemometer for Velocity Measurements

Constant temperature anemometry (CTA) method is used for the measurement of the fluctuating velocity. This method is used widely for the transfer function measurements ([14], [21], [22], [30], [32]). The working principle is based on the cooling effect

of a flow on a heated wire, where the wire is kept at constant temperature by changing the current through it. The circuit diagram of a constant temperature anemometer can be seen in Figure 3.3. The wire (R_w) is connected to one arm of a Wheatstone bridge and heated by an electrical current, where a servo amplifier keeps the bridge in balance by controlling the current to keep the temperature constant. The bridge voltage (E) represents the heat transfer, where the convective heat transfer from the wire is a function of flow velocity. Therefore, the bridge voltage is a direct measure of the velocity.

In the experiments, a Dantec Dynamics MiniCTA hot-wire anemometer with probe 55P11 is used. The probe has 5 μm diameter and 1.25 mm long platinum-plated tungsten wire sensors. This wire probe is inserted on the tube with a 4 mm thick probe holder, by aligning the wire sensor perpendicular to the flow.

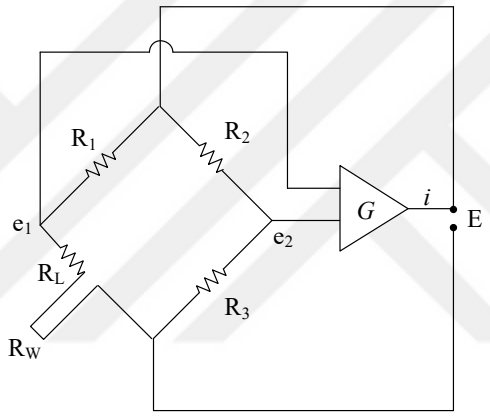

Figure 3.3. Constant temperature anemometer circuit diagram

3.1.3. Chemiluminescence Measurements

In order to determine the heat release rate fluctuations, chemiluminescence intensity of CH* radicals is measured with a photomultiplier tube. A typical photomultiplier tube consists of 4 main parts: Photoemissive cathode, focusing electrodes, electron multiplier and electrode collector (anode) in a vacuum tube. After the light enters the photoemissive cathode, it emits the photoelectrons into the vacuum. Then, the focusing electrode voltages directs the photoelectrons to the electron multiplier where they are multiplied by

a secondary emission process. The multiplied electrons are collected by the electron collector as output voltage signals, which represents the chemiluminescence intensity.

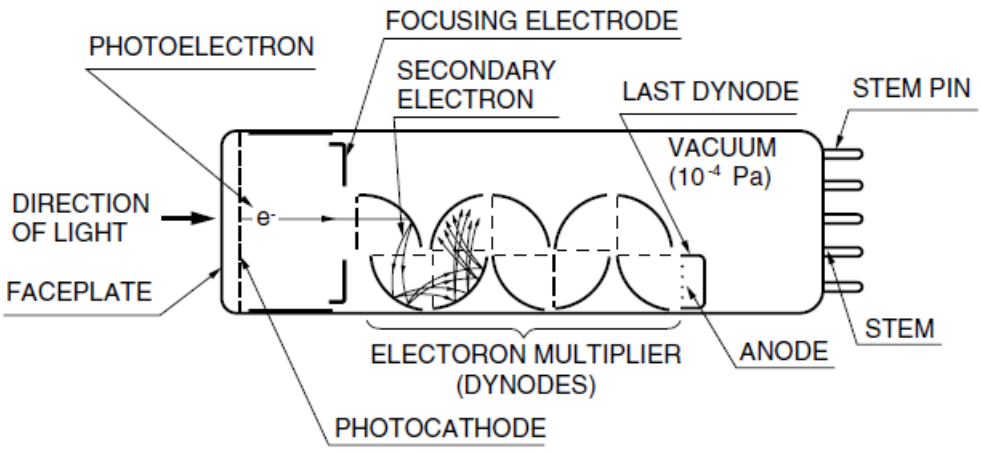

Figure 3.4. Photomultiplier tube

The correlation between the chemiluminescence of various radicals and heat release rate are studied in the literature and widely accepted for the measurement of the flame transfer function (see Section 2.6). In this study, Hamamatsu C6271 photomultiplier tube socket assembly is used with a photomultiplier tube (R3788) where the peak wavelength is at 420 nm. The photomultiplier tube is selected for the measurement of the heat release oscillations, since it has a low signal to noise ratio at these wavelengths.

3.1.4. Mass Flow Controllers

For the controlling of the gas and mixture flow rate, Bürkert Type 8626 mass flow controller and Type 2300 angle-seat control valve are used. The mass flow controllers are operated via an in-house built software of the test rig, where the power supplied to the burner can be monitored as well. (Figure 3.5).

3.1.5. Loudspeaker and Waveform Generator

The fuel/air mixture is perturbed with a loudspeaker, which has a frequency response between 30 Hz and 25 kHz. The required perturbation amplitude and frequency

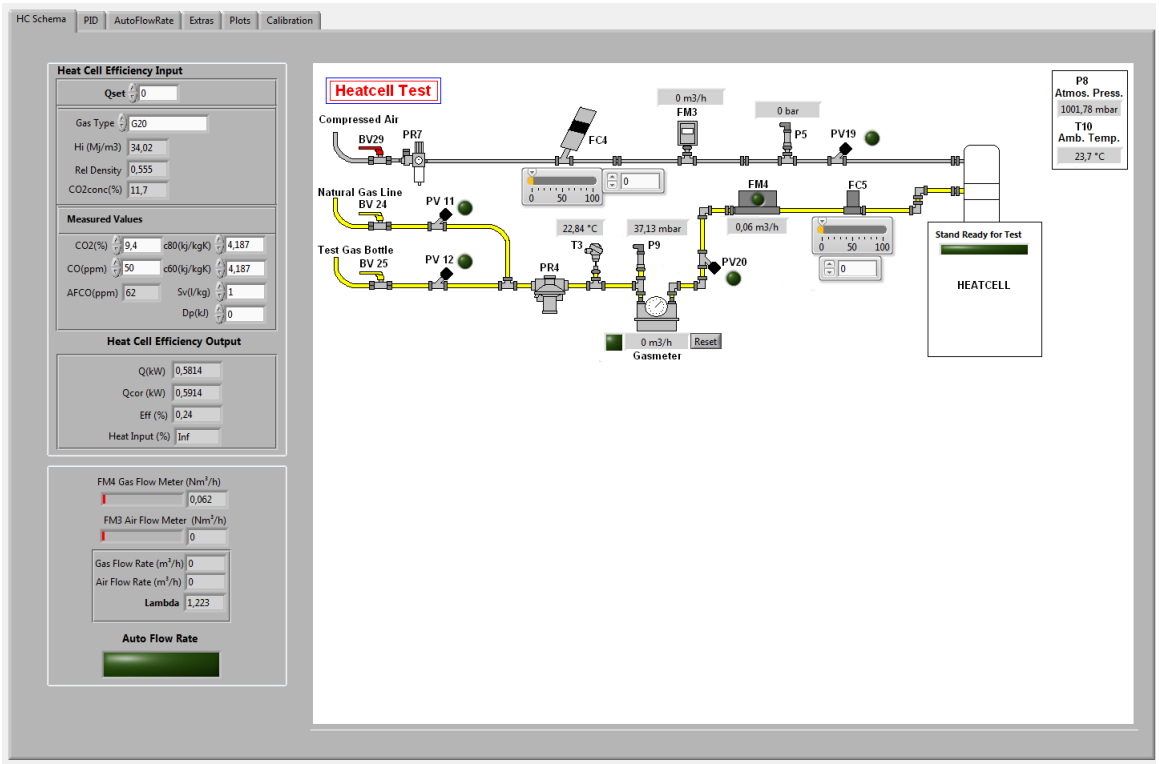

Figure 3.5. Software interface of the mass flow controllers

is adjusted via Agilent 33521A Waveform Generator. The perturbation level is measured with a microphone from the upper end of the aluminium tube, in order to represent the perturbation amplitude in sound pressure level.

3.1.6. Data Acquisition

The voltage signals from the photomultiplier tube and the hot-wire anemometer are converted from analog to digital signals via National Instruments NI-9215 data acquisition card, which has 4 channels, 16-bit resolution, ± 10 V input range and 10 kS/s sampling rate (Figure 3.6). The raw experimental data are recorded at a sampling rate of 10 kHz with 0.5 s time history.

A special script is written in LabView, in order to record the voltage signals through the data acquisition card and visualize them on time and frequency domain (Figure 3.7).

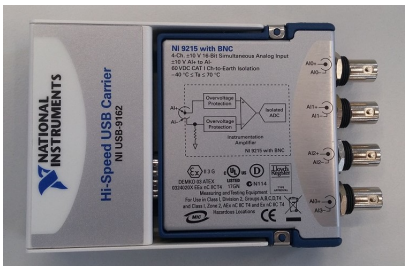

Figure 3.6. National Instruments data acquisition card

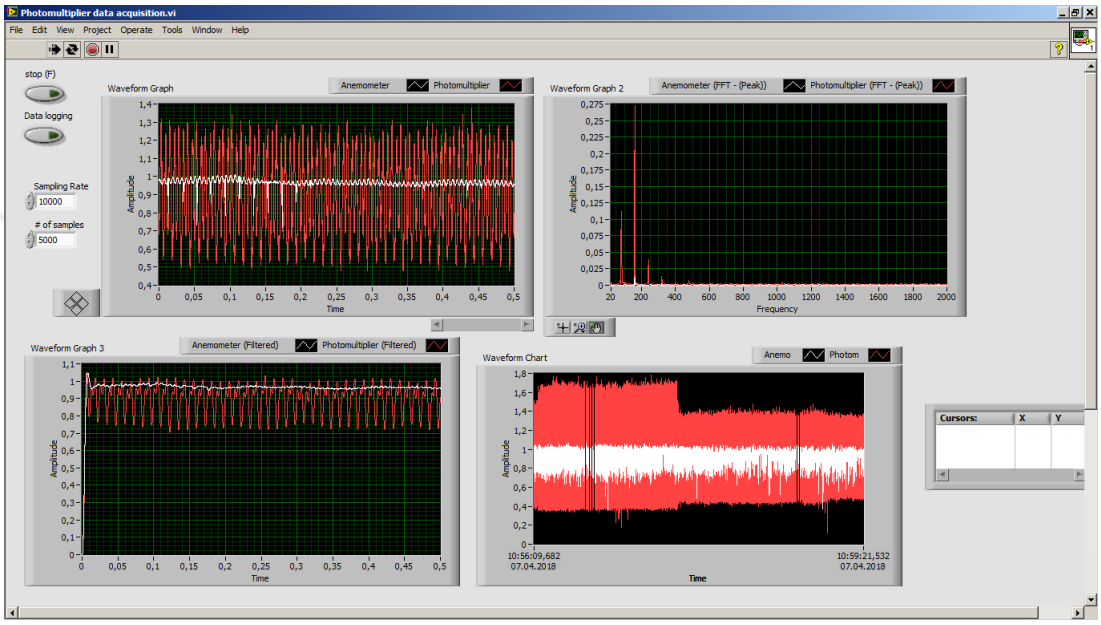

Figure 3.7. Data acquisition interface

3.2. Operation of the Experimental Setup

The required air and fuel for the combustion are fed downstream of the tube, where it is adjusted with the mass flow controllers. At the same time, the igniter, which is located near the burner surface, is operated. At the moment when the fuel-air mixture reaches to the burner, required energy for ignition is supplied with a spark from the igniter and the flame is formed on the burner surface. After the flame is attached on the burner, the loudspeaker is turned on in order to create the flow perturbations. After the required fuel-air mixture rate and required frequency and amplitude for the perturbation are adjusted, and the hot-wire anemometer and the photomultiplier tube are turned on, the setup is ready for the measurement. From the LabView interface, data logging is started

and measurements are done for the instantaneous flow perturbations from the hot-wire anemometer and corresponding flame response from the photomultiplier tube by means of instantaneous heat release rate. Figure 3.8 shows the velocity and heat release rate oscillations from hot-wire anemometer and photomultiplier tube signals. This procedure is repeated for each perturbation frequency between 100 Hz and 1000 Hz, which is the interested range. Even though the frequency response of the loudspeaker is claimed to start from 30 Hz, the loudspeaker could not be able to produce clear tone at frequencies lower than 100 Hz. Therefore no measurements were conducted at frequencies lower than 100 Hz.

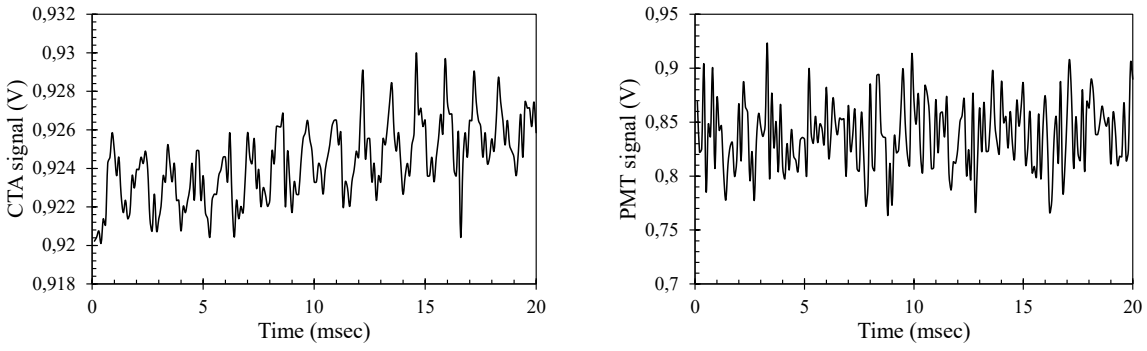

Figure 3.8. a) CTA and b) PMT signals for f=800 Hz perturbation

3.3. Data Processing and Calculation of the Flame Transfer Function

The gain of the flame transfer function is the ratio of the relative magnitude of the system output to the relative magnitude of the system input. In this case, it is the ratio of the heat release rate to the velocity oscillations:

$$Gain = \frac{q'(t)/\overline{q}}{u'(t)/\overline{u}} \tag{3.1}$$

The gain obtained in Eq. 3.1 is the ratio of the voltage signals of hot-wire anemometer and photomultiplier tube, which is an arbitrary value. In order to normalize the transfer function, the quasi-steady response is used. If there is no perturbation, the gain equals to

1, since the input and the output are same, with a zero phase lag. Therefore, the obtained value can be used as the normalization factor for the other excitation frequencies.

The transfer function phase is defined as the phase difference between heat release oscillation ($q'(t)$) and flow velocity oscillation ($u'(t)$). The phase is calculated by making a cross-correlation analysis of these two signals, which is the integral measure of the similarity between the signals $q'(t)$ and $u'(t + \mathbb{T})$:

$$CC(\mathbb{T}) = \frac{1}{T} \int_0^T q'(t)u'(t + \mathbb{T})dt \tag{3.2}$$

In the cross-correlation analysis, the time lag $\mathbb{T}$ is obtained where the $CC(\mathbb{T})$ has the first maximum. After the time lag is found, the phase lag is calculated by $\tau = 2\pi f \mathbb{T}$. Since the cross-correlation function uses all measured data, the influence of the noise on the signal is suppressed. Therefore, it is an accurate method of the phase lag measurement.

After the measurement of the heat release rate and the velocity, the raw experimental data are processed with a script written in MATLAB to calculate the flame transfer function gain and phase, as explained in this section. In Figure 3.9 an example representation of the gain and phase of the flame transfer function is depicted.

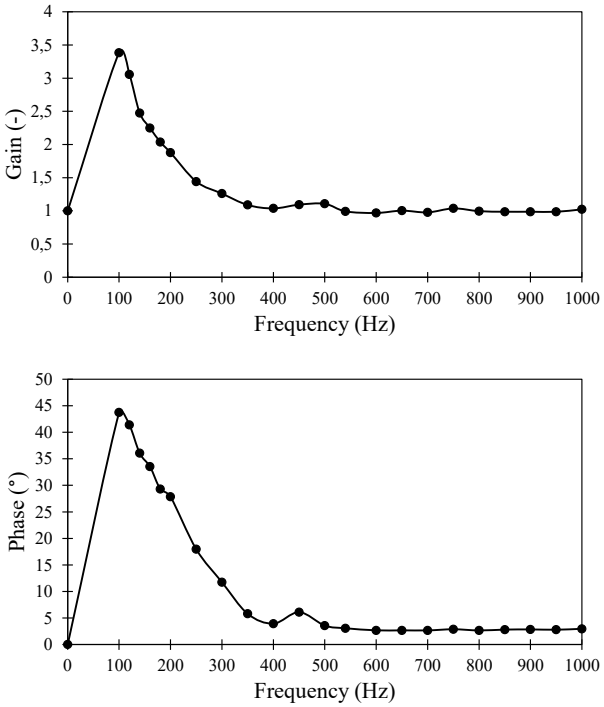

Figure 3.9. Example representation of the flame transfer function

3.4. Experimental Matrix

A series of parametric studies are conducted experimentally. In Table 3.1, the experimental matrix is given. Test no.1 is taken as reference for the rest of the tests as comparison. First, the effect of the equivalence ratio is studied in Test no.2 and 3. Similarly, the effects of the limit gases are studied in Test no.4 and 5. In Test no.6 and 7, the effects of different perturbation amplitudes are investigated. In Test no.8 and 9, different burner samples from different suppliers are compared. Finally, in Test no.10 and 11, the effect of the inner distributor in burner sample no.1 is investigated.

Table 3.1. Experimental matrix

Test no.	Burner sample no.	Equivalence ratio (ϕ)	Gas type	Perturbation amplitude (dB)	Additional part in burner
1	1	0.75	G20 (100% CH_4)	92	Inner distributor
2	1	0.67	G20 (100% CH_4)	92	Inner distributor
3	1	0.82	G20 (100% CH_4)	92	Inner distributor
4	1	0.75	G21 (87% CH_4 + 13% C_3H_8)	92	Inner distributor
5	1	0.75	G23 (92.5% CH_4 + 7.5% N_2)	92	Inner distributor
6	1	0.75	G20 (100% CH_4)	80	Inner distributor
7	1	0.75	G20 (100% CH_4)	86	Inner distributor
8	2	0.75	G20 (100% CH_4)	92	-
9	3	0.75	G20 (100% CH_4)	92	-
10	1	0.75	G20 (100% CH_4)	92	-
11	1	0.75	G20 (100% CH_4)	92	Inner distributor + Plus shape

CHAPTER 4

RESULTS AND DISCUSSION

In this chapter, the results of the experimental study of the flame transfer function are presented. The flame response of the burners used in domestic condensing boilers is measured. A parametric investigation is conducted in order to show the effects of the burner and flame parameters on the flame transfer function, which includes the influence of the equivalence ratio ϕ, the limit gases, perturbation amplitude, burner types from different manufacturers and burner with different distribution plates.

In Section 4.1, the effect of the mixture equivalence ratio on the flame transfer function is discussed, where the flame transfer functions of three different equivalence ratios are compared. Section 4.2 reports the influence of the limit gases of methane on the flame transfer function. In Section 4.3, the effects of different perturbation amplitudes on the flame response are discussed. The comparison between the flame transfer functions of the burner samples from different manufacturers is presented in In Section 4.4. Finally, the effect of two different distributor plates on the flame transfer function is studied in Section 4.5. All of the tests are conducted at a power of 2.5 kW, where the gas flow rate is 3.76 m^3/h. The effects of the equivalence ratio, the limit gases, the perturbation amplitude and the distributor plate on the flame transfer function are measured with burner sample no.1.

4.1. Effects of the Mixture Equivalence Ratio

The equivalence ratio is one of the most important parameters for flame characterization. It is defined as the ratio of the actual fuel-to-air ratio to the stoichiometric fuel-to-air ratio and shown with the symbol of ϕ. In general, if the actual fuel-to-air ratio is lower than stoichiometric ratio ($\phi < 1$), these mixtures are considered lean mixture. As explained earlier, the concept of lean premixed combustion is adopted in domestic condensing boilers, due to environmental concerns. For the low loads (< 8 kW), the equivalence ratio is around $\phi = 0.75$ for most of the condensing boilers. In this section,

the effects of changing equivalence ratios are investigated at 3 different equivalence ratios of $\phi = 0.67, 0.75$ and 0.82 and the results are presented in Figure 4.1.

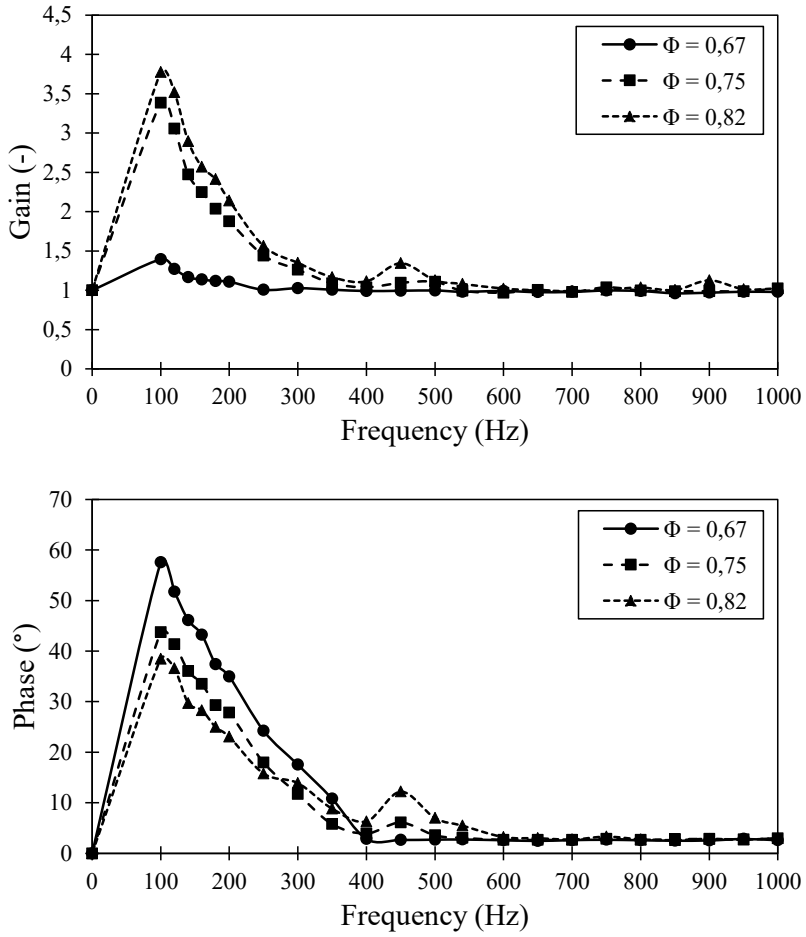

Figure 4.1. Gain and phase of the flame transfer function for burner sample no.1 at different equivalence ratios and perturbation level of 92 dB

The gain of the transfer function shows peaks for each 3 cases at 100 Hz, where this is the critical region for the resonance. This means that the flame response is such strong at 100 Hz, that the flame can drive an instability at this frequency. From the results, it can be seen that the gain of the transfer function increases with increasing equivalence ratio at 100 Hz. A change in the equivalence ratio affects the burning velocity, which results a variation in the flame. As the mixture equivalence ratio is increased, the burning velocity increases, resulting lower flame height. In this case, the flame stabilizes closer to the burner surface (as shown in Figure 4.2) and burner surface temperature increases agreeing with previous studies [21]. If the mixture's equivalence ratio is decreased, this

time the flame height increases and since the flame moves away from the burner, the burner surface temperature decreases. Considering these results, for 100 Hz frequency, the gain of the transfer function increases with decreasing flame height. There is also a slight increase in gain for $\phi = 0.82$ at 450 and 900 Hz, which shows that flame could drive an instability at those frequencies. These areas might need more investigation while using this burner in the boiler.

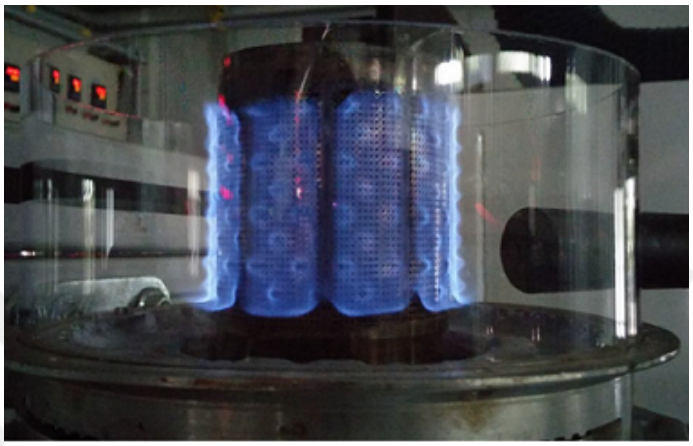

a)

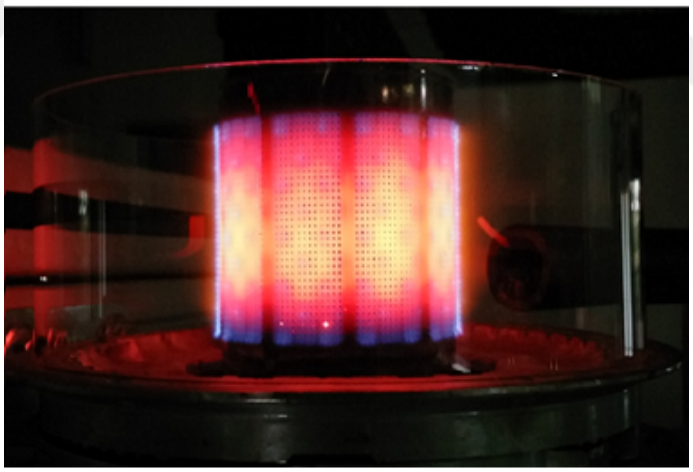

b)

Figure 4.2. Flame at the equivalence ratio of a) $\phi = 0.67$ and b) $\phi = 0.82$

The variation in the equivalence ratio has an effect on the phase of the transfer function as well. The phase shows an increasing behaviour when the equivalence ratio tends to go to the leaner side. This behaviour could be attributed to the higher flame

length at lower equivalence ratios. Since the burning velocity decreases, flame height increases and this causes higher time lag for the perturbations to reach from the burner surface to the flame [30].

In Figure 4.2, the visuals of the flames at the equivalence ratio of $\phi = 0.67$ and 0.82 can be seen. At $\phi = 0.67$, the flame height is higher and the flame is close to the blow-off limit (when the flame will separate as the velocity gets higher than the rate of propagation). The flame lift can be clearly seen, where the flame hardly stabilized on the burner surface. The flame behaviour changes at $\phi = 0.82$. Since the burning velocity is higher, the flame height is lower. Therefore, the burner surface temperature is higher compared to lower equivalence ratios. The high surface temperatures can be seen from glowing perforation material as well. If the equivalence ratio is increased much higher levels, the burning velocity will be greater than the mixture velocity after some level and the flame will blow-off.

4.2. Effects of the Limit Gases

In the boiler development, manufacturers must comply with the related standards, which include the limit conditions that boiler could operate. One of those standards is BS EN 437, which specifies the test gases of the appliances that burning gaseous fuels of the first, second and third families. In this standard, gases are classified into three families, where methane is the reference gas of the second family and designated as G20. This standard includes the representatives of the extreme variations in the content of the gases as well, which are designated as limit gases. Limit gases simulate the conditions in the field, where a boiler must operate safely, without any deterioration. G21 is the incomplete combustion limit gas of second family, which contains 87% methane (CH_4) and 13% propane (C_3H_8) by volume. This limit gas could be encountered in field during winter season, where propane is mixed for increasing the calorific value of the natural gas. The other limit gas is G23, the flame lift limit gas, which contains 92.5% methane and 7.5% nitrogen (N_2) by volume. This low calorific value gas could be encountered in some countries in Europe.

The behaviour of the limit gases are similar to different mixture equivalence ratios. For G21 case, since its calorific value is higher than G20 (methane) where the gas contains

more hydrocarbons, it can be compared to high equivalence ratio mixtures (rich mixtures). On the other hand, for G23 case, it can be compared to low equivalence ratio mixtures (lean mixtures).

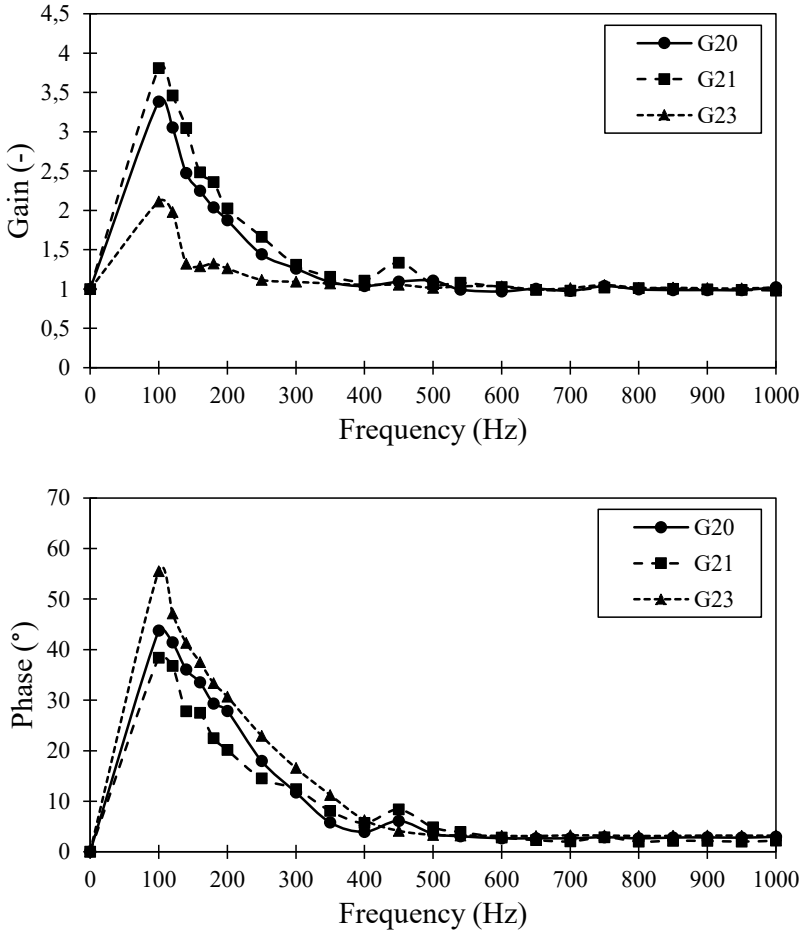

Figure 4.3. Gain and phase of the flame transfer function for burner sample no.1 with methane and its limit gases at the perturbation level of 92 dB, $\phi = 0.75$

In this section, the effect of the limit gases on the flame transfer function is investigated. The results are shown in Figure 4.3. The gain of the transfer function shows similar behaviour to the gain values of different mixture equivalence ratios. 100 Hz frequency region is critical for the establishment of a resonance. With G21, the burning velocity is high, therefore the flame height is low and the flame attaches to the burner surface closely, which brings the high burner surface temperature. With G23, the gain of the transfer function acts as low mixture equivalence ratio case, since its methane content is lower than G20 and there is no other hydrocarbon inside. Since the burning velocity

decreases, the flame height gets higher and the flame moves away from the burner surface. Therefore, the burner surface temperature decreases. From the results, it can be seen that the gain of the transfer function decreases with the test gas gets leaner at 100 Hz, as expected. Same peaks in the gain is observed at 450 Hz with G21, as seen in high mixture equivalence ratio.

The phase of the flame transfer function shows similar behaviour with varying mixture equivalence ratios as well. The phase is increasing at 100 Hz frequency, with G23 gas where the mixture is leaner. This is based on the same reason with lower mixture equivalence ratio case where the perturbations delay to reach from the burner surface to the flame, since the flame height increases.

Apart from these analysis of the limit gases, it is important to highlight that the limit gases contain different components other than methane and consequently it could affect the heat release rates and burner surface temperatures. Therefore, the thermoacoustic behaviour of the flame might change slightly. For this reason, a more detailed scan might be required when the burner is used in the boiler.

4.3. Effects of the Perturbation Amplitude

The required perturbation to the mixture flow is supplied with a loudspeaker. In order to increase the amplitude, an amplifier is connected to the loudspeaker and the required perturbation frequency and amplitude are adjusted via a waveform generator. By the nature of the flame transfer function, it is required to perturb the mixture flow at different frequencies within the interested range. So that, the behaviour of the gain and the phase of the transfer function could be seen in that range. On the other hand, the reason to perturb the mixture flow at different amplitudes is slightly different. In reality, the burner operates within a closed vessel. In this case, it is within the heat cell of a boiler. Naturally, the components inside the heat cell affect the acoustics of the system by creating pressure fluctuations, e.g. the fan could create such pressure fluctuations at its blade pass frequency while running at a specific speed. In this case, when the flame response is high against these perturbations, resonance might occur within the system. The reason to perturb the mixture at different amplitudes is to investigate the flame response against different flow perturbations caused by the system acoustics. In this test series, 3 perturbation levels are

studied. The perturbation levels are measured as sound pressure level with a microphone at the burner outlet, where these perturbation levels are 80, 86 and 92 dB.

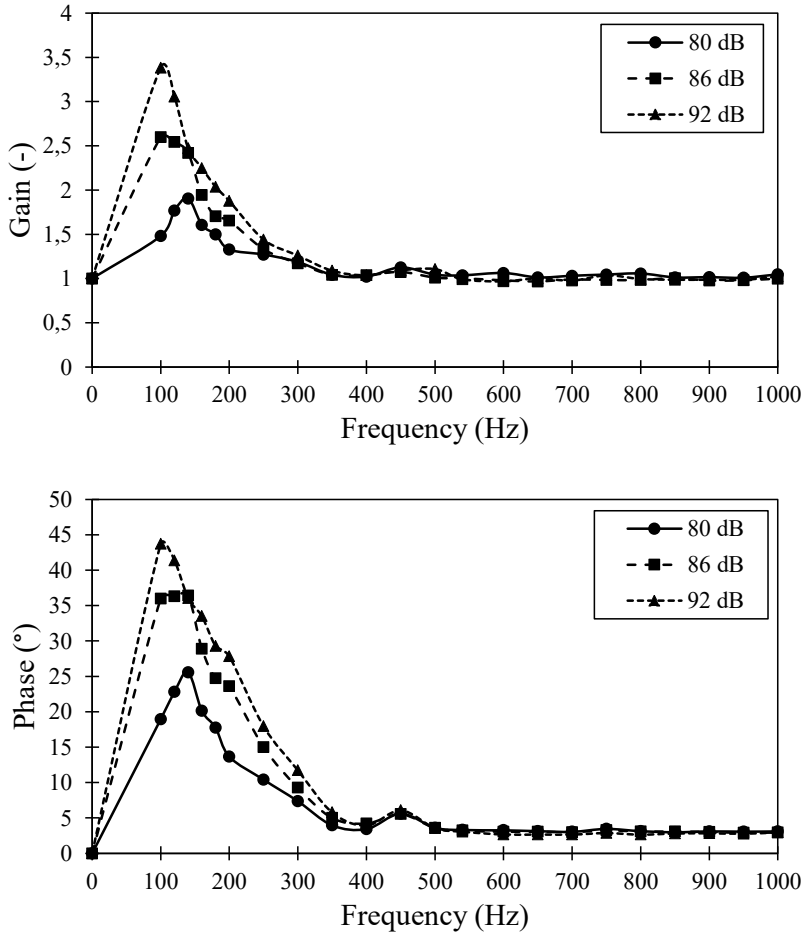

Figure 4.4. Gain and phase of the flame transfer function for burner sample no.1 at different perturbation levels, $\phi = 0.75$

The effects of different perturbation amplitudes are investigated and the results are shown in Figure 4.4. For the three perturbation levels, the gain is maximum at 100 Hz. At low frequencies, flame acts as an amplifier and the gain is higher than 1. The gain increases with increasing perturbation level up to 350 Hz. Considering the decreasing trend in the gain at 100 Hz with a decrease in perturbation level, resonance might not occur below 80 dB perturbation level. In high frequencies, the gain saturates, where the flame can hardly drive an instability with these three perturbation levels at higher frequencies than 350 Hz. Figure 4.4 also shows that the phase of the transfer function is very low as long as the perturbation frequency is beyond 500 Hz, independent from the perturbation level.

At lower frequencies, the phase shows an increase as the perturbation level increases. This behaviour could be attributed to the increased time lag for the incoming perturbations to reach the flame when the perturbation amplitude becomes large [24]. There is a slight increase in phase at 450 Hz, where the flame might not drive an instability by itself. However, this frequency could be problematic due to the acoustic characteristics when the burner is used in a boiler.

4.4. Effects of the Different Burner Samples

The burner is the most important component within a heat cell regarding thermoacoustic behaviour. Burners that are used in premixed systems, in this case in the condensing boilers, generally consist of perforated burner decks with different hole and slot patterns. One of the design parameter for a thermoacoustically stable burner is the combination of the holes and slots, and their sizes as well. Since there is an endless variation in those combinations, burner manufacturers must design the perforation pattern in a way that the flame response to the acoustic perturbations are minimum. In addition to the perforation pattern, the burner inlet geometry has an effect on the thermoacoustic behaviour in some cases. However, the studies in the literature have only focused on the effects of different perforation patterns by several researchers ([14], [22], [32]).

In this section, the difference in the flame transfer function of three types of burner samples are investigated. The investigated burner samples are shown in Figure 4.5. The equivalence ratio ($\phi = 0.75$) and the perturbation amplitude (92 dB) are kept constant.

All of the three burners have similar porosity, where sample no.1 consists of only holes, sample no.2 has separate hole and slot lines and sample no.3 includes a mixed pattern of holes and slots. Results of the comparison of the flame transfer function for three different burners are shown in Figure 4.6. As expected, there are big differences in gain between different perforation patterns. The gain of the flame transfer function shows peaks at different frequencies, which can be explained as burners have a sensitivity against flow perturbations at different frequencies. This means that resonance might occur for sample no.1 at 100 Hz, for sample no.2 at 300 Hz and between 450 and 500 Hz, for sample no.3 at 550 Hz. This behaviour is discussed in [32], where it is stated that in case of multiple flames, the interaction between adjacent flames could affect the flame

a) b)

c)

Figure 4.5. Burner samples with different perforation patterns a) Sample no.1, b) Sample no.2, c) Sample no.3

parameters where the flame transfer function could depend on the perforation pattern. The perforation pattern is an essential parameter for the flame height as well. With a variation in flame height, the phase delay changes as happened in this case. As explained in previous sections, when the flame stabilized on the burner away from the surface, which means flame height is higher, there will be a higher time lag between velocity and heat release rate perturbations since it will take more time for the perturbations to reach from the burner surface to the flame. Visual inspections have good agreement with the phase results, where sample no.1 has highest flame length and sample no.2 has the lowest. This behaviour can be explained as the sample no.2 has more slots than the other two burners,

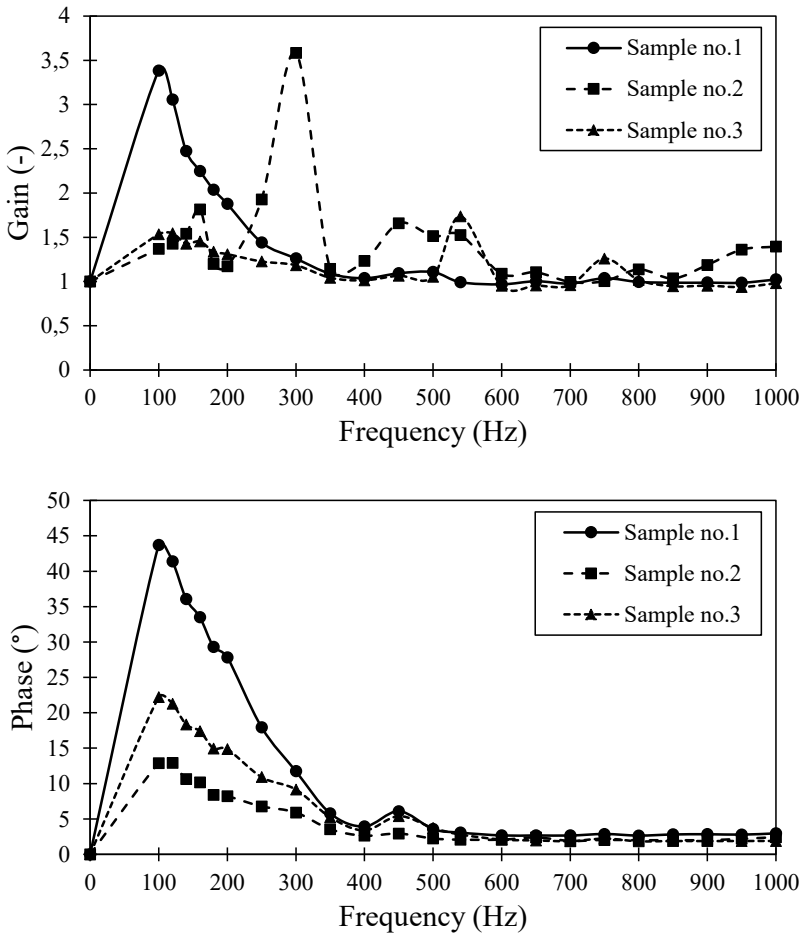

Figure 4.6. Gain and phase of the flame transfer function for different burner samples at the perturbation level of 92 dB, $\phi = 0.75$

which leads to an increase of the area that fuel/air mixture flows, compared to the holes. This means that the mixture flow velocity will decrease and consequently the burning speed increases, which leads to lower flame height.

4.5. Effects of the Distributor Plates

The cylindrical perforated plate burners used in the boilers are the components that consist of an inlet cone where the fuel/air mixture coming in, a cap closed at lower end, and a cylindrical perforated plate around where flame is attached. In some combustors, it is necessary to add additional parts in order to distribute the mixture through the surface of the burner evenly. Otherwise, since the mixture is not evenly distributed, the flame

height may be differ through the circumference of the surface. In this case, one of the concern is that the flame height will increase such levels where it will interact with the combustor walls and consequently the CO emissions could exceed the legal limits. The other concern, which is investigated in this study, since the flame length could be different then the flame response of the burner could vary. In this section, the effect of different distributor plates on the flame transfer function is studied.

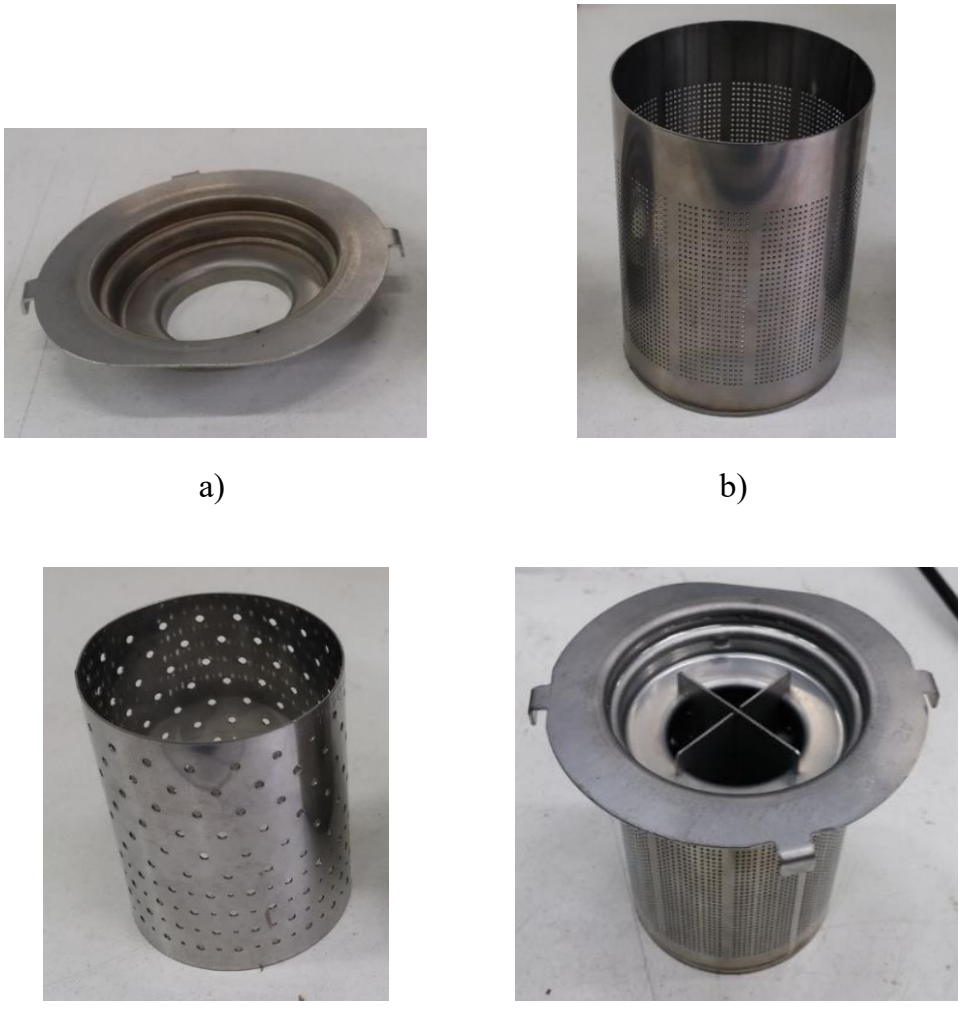

a) b)

c) d)

Figure 4.7. Parts of the burner a) Inlet cone, b) Burner deck, c) Inner distributor, d) Cross part

In order to achieve a uniform flow through all burner surface, two different distributors are introduced, which are shown in Figure 4.7c and 4.7d. The distributor in Figure 4.7c is designated as inner distributor and it is a part of the burner sample no.1. Normally, it is positioned inside the burner deck (Figure 4.7b). The "cross part" (Figure 4.7d) is placed on top of the inlet cone, just to compare the effects on the flame transfer function and to check if the flame response is affected.

In this test series, there are three configurations tested. The first one is with the original configuration of the burner sample no.1 (a+b+c). The second configuration is the burner sample no.1 without inner distributor (a+b). The third configuration is, the addition of cross part to burner sample no.1 (d).

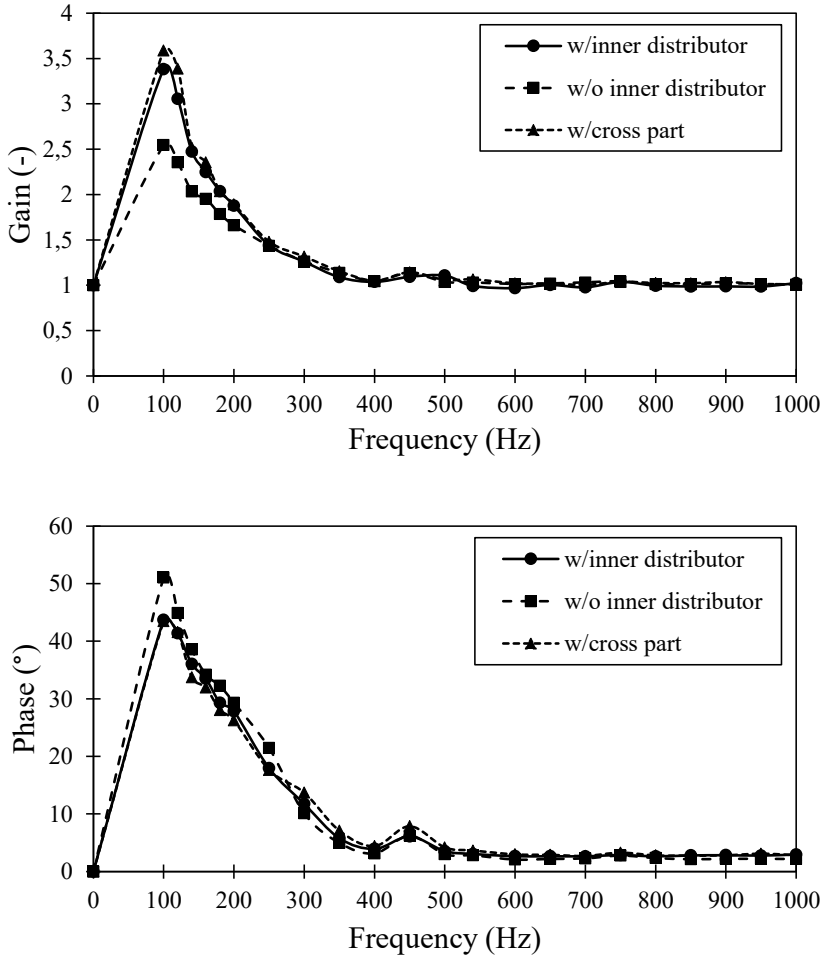

Figure 4.8. Gain and phase of the flame transfer function for the burner sample no.1 with and without distributors at the perturbation level of 92 dB, $\phi = 0.75$

In Figure 4.8 the results are presented for the flame transfer function of the burner samples with different distributor plate configurations. The effect of the presence of inner distributor can be seen from the increase in gain. This behaviour could be attributed to the difference in mixture velocity. In the absence of the inner distributor, the mixture is not evenly distributed and the flame length vary in the whole perforation. In this case, the flame length which corresponds to the measurement point of photomultiplier, is higher. Therefore, the gain decreases in the burner without inner distributor. The phase is highest in the same case at 100 Hz, which can be explained with higher flame length in the absence of inner distributor. There is no significant change observed for the cross part on gain and phase of the flame transfer function. The cross part has no use in this frequency and power range regarding thermoacoustic behaviour.

4.6. Summary

In this chapter, the experimental study of the flame response of the burners used in domestic condensing boilers was presented. The effects of flame and burner parameters on the flame transfer function were shown. It was proven that the studied parameters (equivalence ratio, limit gases, perturbation amplitude, burner types) have a big influence on the flame, consequently on the combustion stability within the system. This is an important finding for the thermoacoustic instability analysis of the boilers, which could save significant amount of time and effort during the development of a new system.

Overall, it could be seen that burner sample no.1 had a vulnerability to the thermoacoustic instabilities at low frequencies. By changing the flame parameters such as equivalence ratio, it was shown that this vulnerability could be changed as well. Similar to the effect of the equivalence ratio, the flame response changed at the limits of the operational range of the boiler with limit gases. This result showed that the flame can be more vulnerable to the resonances with limit gas. From the flame transfer function graphs, the effects of different perturbation amplitudes showed that if there is a change in the acoustic system, the flame amplifies those perturbations at different levels. It was also proven that different burners have different flame response, therefore it can be said that the sensitivity of the flame to the thermoacoustic instabilities were mostly dependent on the burner design. This study also showed that implementation of additional parts to the

burner might have an effect on the flame response by changing the flame distribution and length.

Considering these results, if the flame characterization of the burner samples were performed before the development tests in the boiler, the frequencies at which the flame could amplify could be seen. If those frequencies are close to the eigenfrequency of the system, this means the flame will amplify those frequencies and the system will resonate. In order to avoid them, design modifications in the burner could be made in the early stages of the development or a Helmholtz resonator could be designed accordingly. With this approach, by making the flame characterization firstly, the development time and effort could be reduced significantly in the design phase.

CHAPTER 5

CONCLUSION AND FUTURE WORK

In this study regarding the thermoacoustic instabilities in domestic condensing boilers, it was aimed to get more insight in the flame response to the acoustic oscillations in a boiler system. The flame characterization of perforated plate burners normally used in domestic condensing boilers was studied. For this purpose, experiments were performed to determine the flame transfer function between the acoustic velocity of the fuel/air mixture and the heat release rate of the flame. In order to conduct the tests, an experimental setup was built based on methods reviewed in the previous studies. For the velocity measurements, a hot-wire anemometer was used and for the heat release rate measurements, a photomultiplier tube was used. After post-processing the experimental data, the flame transfer function was obtained for different conditions. The effects of different flame and burner parameters on the flame transfer function were investigated and the results can be summarized as follows:

First, the effect of the equivalence ratio of the fuel/air mixture on the flame transfer function was studied. It was observed that with increasing equivalence ratio, the flame height decreased due to the higher burning velocity. Similarly, higher gain values were obtained at higher equivalence ratios. The phase showed an increasing trend with decreasing equivalence ratios, because of the larger time lag for the perturbations to reach to the flame. Similar observations were made for the limit gases of methane, where the critical frequency was same. With G21, the flame height was low because of the high burning velocity. On the other hand, the flame height was higher for G23, where the phase of the flame transfer function was the highest. These results showed that the fuel/air ratio of the mixture and the content of the fuel has an important effect on the flame and consequently on the flame transfer function. After investigating the flame parameters, the effect of different perturbation amplitudes were studied in order to observe the sensitivity of the flame response to the perturbations caused by the system acoustics. The results show that the gain and phase both increased with increasing perturbation amplitude. From these results, it can be concluded that flame response changes with different flow perturbations. The flame transfer function was also compared for different burner samples, i.e. different

perforation patterns. The influence of the perforation pattern showed itself in the gain, where each burner had a sensitivity at different frequencies. These results showed that the change in the perforation pattern, changes the flame characteristics significantly. Lastly, the effect of the distributor plates of the burner was investigated. Inner distributors provide an even flow distribution through the burner surface. When it is extracted from the burner, the mixture is not evenly distributed and the flame height varies through the perforation. Therefore, the flame transfer function changes as well. There was no effect of the cross part found on the flame transfer function within the scanned frequency and power range. From all test results, it was observed that 100 Hz is critical for the burner sample no.1, for the occurrence of a resonance, where it was also seen that changing the flame and burner parameters had an effect on the occurrence.

This study presented the flame characterization of a burner where the effects of various flame and burner parameters on the flame response, which contributes to the prediction of thermoacoustic instabilities, were investigated. By changing these parameters, especially the perforation pattern, a desired flame could be achieved. This approach helps the developer to foresee the resonances in very early development stages, by showing the susceptibility of the flame to the acoustic perturbations within the system, where the flame could amplify the instabilities. However, the flame characterization alone does not provide exact prediction of the thermoacoustic instabilities. In order to predict the thermoacoustic instabilities of a system, the Rayleigh index must be found (Eq.2.1), which requires the acoustic properties of the system. For the future studies, the thermoacoustic stability analysis of the system should be done by making the acoustic characterization of the system and using this investigation as an input for flame characterization. In addition, the flame characterization could be extended to higher operational power ranges of the boiler.

REFERENCES

[1] B. Higgins, “On the sound produced by a current of hydrogen gas passing through a tube”, *J. Nat. Phil., Chem., and the Arts 1* 183(6), pp. 129–131 (1802).

[2] P. L. Rijke, “Notiz über eine neue Art, die in einer an beiden Enden offenen Röhre enthaltene Luft in Schwingungen zu versetzen”, *Annalen der Physik* 183(6), pp. 339–343 (1859).

[3] Lord Rayleigh, “The explanation of certain acoustical phenomena”, *Nature* 18, pp. 319–321 (1878).

[4] A. Putnam and W.R. Dennis, “Burner oscillations of the gauze tone type”, *The Journal of the Acoustical Society of America* 26(5), pp. 716–725 (1954).

[5] D. Fritsche, *Origin and Control of Thermoacoustic Instabilities in Lean Premixed Gas Turbine Combustion*, PhD thesis, Swiss Federal Institute of Technology Zurich (2005).

[6] J.P. Hathout, “Thermoacoustic instability”, In *Fundamentals and Modeling in Combustion, 2.280*. Reacting Gas Dynamics Computational Lab, Department of Mechanical Engineering, MIT, Cambridge (1999).

[7] A.P. Dowling and J.E. Ffowcs Williams, *Sound and Sources of Sound*, Ellis Horwood Limited, West Sussex, England (1983).

[8] W. Polifke, “Combustion instabilities”, *von Kármán Institute Lecture Series* (2004).

[9] V.K. Khanna, *A Study of the Dynamics of Laminar and Turbulent Fully and Partially Premixed Flames*, PhD thesis, Virginia Polytechnic Institute and State University (2001).

[10] P. Riess, “Das Anblasen offener Röhren durch eine Flamme”, *Annalen der Physik* 184(12), pp. 653–656 (1859).

[11] P. Riess, “Anhaltendes Tönen einer Röhre durch eine Flamme”, *Annalen der Physik* 185(1), pp. 145–147 (1860).

[12] R.L. Raun, M.W. Beckstead, J.C. Finlinson, and K.P. Brooks, “A review of Rijke tubes, Rijke burners and related devices”, *Progress in Energy and Combustion Science* 19(4), pp. 313 – 364 (1993).

[13] J.A. Carvalho, M.A. Ferreira, C. Bressan, and J.L.G. Ferreira, “Definition of heater location to drive maximum amplitude acoustic oscillations in a Rijke tube”, *Combustion and Flame* 76(1), pp. 17 – 27 (1989).

[14] V.N. Kornilov, *Experimental Research of Acoustically Perturbed Bunsen Flames*, PhD thesis, Eindhoven University of Technology (2006).

[15] M. Fleifil, A.M. Annaswamy, Z.A. Ghoneim, and A.F. Ghoniem, “Response of a laminar premixed flame to flow oscillations: A kinematic model and thermoacoustic instability results”, *Combustion and Flame* 106(4), pp. 487 – 510 (1996).

[16] P.L. Blackshear, “Driving standing waves by heat addition”, *Symposium (International) on Combustion* 4(1), pp. 553 – 566 (1953).

[17] S. Ducruix, D. Durox, and S. Candel, “Theoretical and experimental determinations of the transfer function of a laminar premixed flame”, *Proceedings of the Combustion Institute* 28(1), pp. 765 – 773 (2000).

[18] T. Schuller, S. Ducruix, D. Durox, and S. Candel, “Modeling tools for the prediction of premixed flame transfer functions”, *Proceedings of the Combustion Institute* 29(1), pp. 107 – 113 (2002).

[19] A. Cuquel, D. Durox, and T. Schuller, “Theoretical and experimental determination of the flame transfer function of confined premixed conical flames”, In *7th Mediterranean Combustion Symposium, Cagliari, Sardinia, Italy* (2011).

[20] K.R.A.M. Schreel, R. Rook, and L.P.H. De Goey, "The acoustic response of burner-stabilized premixed flat flames", *Proceedings of the Combustion Institute* 29(1), pp. 115 – 122 (2002).

[21] H.M. Altay, S. Park, D. Wu, D. Wee, A.M. Annaswamy, and A.F. Ghoniem, "Modeling the dynamic response of a laminar perforated-plate stabilized flame", *Proceedings of the Combustion Institute* 32(1), pp. 1359 – 1366 (2009).

[22] V.N. Kornilov, M. Manohar, and L.P.H. de Goey, "Thermo-acoustic behaviour of multiple flame burner decks: Transfer function (de)composition", *Proceedings of the Combustion Institute* 32(1), pp. 1383 – 1390 (2009).

[23] V.N. Kornilov, R. Rook, J.H.M. ten Thije Boonkkamp, and L.P.H. de Goey, "Experimental and numerical investigation of the acoustic response of multi-slit bunsen burners", *Combustion and Flame* 156(10), pp. 1957 – 1970 (2009).

[24] D. Durox, T. Schuller, N. Noiray, and S. Candel, "Experimental analysis of nonlinear flame transfer functions for different flame geometries", *Proceedings of the Combustion Institute* 32(1), pp. 1391 – 1398 (2009).

[25] T.P. Clark, "Studies of OH, CH, CO and C2 radiation from laminar and turbulent propane-air and ethylene-air flames", *NACA-TN-4266* (1958).

[26] R.B. Price, I.R. Hurle, and T.M. Sugden, "Optical studies of the generation of noise in turbulent flames", *Symposium (International) on Combustion* 12(1), pp. 1093 – 1102 (1969).

[27] B. Higgins, M.Q. McQuay, F. Lacas, and S. Candel, "An experimental study on the effect of pressure and strain rate on ch chemiluminescence of premixed fuel-lean methane/air flames", *Fuel* 80(11), pp. 1583 – 1591 (2001).

[28] Y. Hardalupas and M. Orain, "Local measurements of the time-dependent heat release rate and equivalence ratio using chemiluminescent emission from a flame", *Combustion and Flame* 139(3), pp. 188 – 207 (2004).

[29] R. Balachandran, B.O. Ayoola, C.F. Kaminski, A.P. Dowling, and E. Mastorakos, "Experimental investigation of the nonlinear response of turbulent premixed flames to imposed inlet velocity oscillations", *Combustion and Flame* 143(1), pp. 37 – 55 (2005).

[30] R.D. Parmar, "Acoustics and thermoacoustics: Transfer matrix approach, characterization of premixed laminar flame", Master's thesis, Otto von Guericke University Magdeburg (2007).

[31] S. A. Reijke, "Thermoacoustic stability analysis of the premixed flame in a compact condensing appliance", Master's thesis, University of Twente (2010).

[32] M. Manohar, *Thermo-acoustics of Bunsen Type Premixed Flames*, PhD thesis, Eindhoven University of Technology (2011).